# Exhibit 118

RJ LEE GROUP
DELIVERING SCIENTIFIC RESOLUTION

August 30, 2019

Mr. Kevin Hynes
Orrick
51 West 52nd Street
New York, New York 10019-6142

Re: Rebuttal of Dr. William Longo's MDL Testing through February 1, 2019.

The purpose of this report is to address the systematic errors made by MAS and specifically Dr. Longo in his analysis of purported Johnson and Johnson Talc powders obtained through the MDL process. I have reviewed reports by Dr. Longo and Dr. Rigler of MAS as well as various deposition and trial testimony as it relates to his testing of the MDL samples produced by Johnson and Johnson. The specific reports I have reviewed are dated: November 14, 2018, January 15, 2019, and February 1, 2019.

In these reports MAS analyzed 56 historic samples of Johnson and Johnson Baby Powder and Johnson and Johnson Shower to Shower products from Johnson and Johnson's historical inventory from over 4 decades. In addition to these 56 samples, an additional 15 samples described as Imerys Railcar samples all have the same systematic errors.

These systematic errors are of critical significance in that they result in misidentification of the species of minerals being observed and the actual morphology of these particles. Thus, because of the deviations taken and expounded below, the methodology employed by Dr. Longo and MAS is incapable of both reliable mineral identification and determination of the asbestiform habit.

**Mineral Identification**

To start we need to define what a mineral is: a mineral is a naturally occurring crystalline solid with a definite, but not necessarily fixed, chemical composition (Nesse 2000).

When discussing the analytical techniques and method below it is important to understand how each instrument measures properties that are either indirectly (PLM) or directly (TEM) related to the determination of the crystalline structure and chemical composition of a discrete particle encountered during the analysis of any talcum powder. The following sections discuss in some depth the key aspects of PLM and TEM and their use in mineral identification.

Furthermore, the geologic conditions which governed the formation of any given talc deposit are unique, and as such, extreme caution needs to be taken when evaluating talcum powders from different mines and/or mining regions in the application of standard testing methodologies. It

should be noted that the testing methodology for both PLM and TEM cited by Dr. Longo in his analysis of the Johnson and Johnson MDL samples, if followed, will enable reliable mineral identification and determination if the observed minerals are the asbestiform varieties of serpentine and amphibole group minerals and thus asbestos. However, each time Dr. Longo and MAS deviated from their cited methodology, the result was a false positive for asbestos.

**Polarized Light Microscopy (PLM)**

Polarized light microscopy is a mature technique that requires an understanding of how light interacts with solid transparent materials and how those materials will systematically affect that light. In order to reliably identify the minerals according to ISO 22262-1 by PLM one must, at a minimum, determine the following six properties (see ISO 22262-1 7.2.3.7.1 through 1.2.3.7.6):

i) Morphology
ii) Colour and Pleochrosim
iii) Birefringence
iv) Extinction Angle
v) Sign of Elongation
vi) Refractive indices

Each of these properties allows for the discrimination of most mineral groups (e.g. talc from amphiboles), and in some instances, species of minerals within a mineral group (e.g. tremolite from anthophyllite). Further, each of these properties are indirect measurements that can be correlated to either the crystal structure (e.g. extinction angle) or composition (e.g. refractive indices) of a given mineral.

The use of refractive index liquids also enables one to screen thousands of discrete particles rapidly and reliably as the use of an appropriate liquid causes minerals with similar refractive indices to exhibit certain diagnostic colors. This is in direct contrast to TEM which cannot discriminate any possible particle type of interest based simply on any feature that is as easy to discern as color.

To expound, the importance of the extinction angle measurement specific to the amphiboles at issue in many of these Johnson and Johnson talcum samples is that the majority of amphibole group minerals belong to the monoclinic crystal system. Examples of such are the amphibole minerals, tremolite and cummingtonite. This is in contrast to the amphibole mineral anthophyllite, which is orthorhombic. The observation of an extinction angle parallel to the elongation of a given suspect amphibole particle identifies it as belonging to the monoclinic crystal system and therefore cannot be the amphibole anthophyllite. In contrast if particles observed only exhibit parallel extinction, even upon rolling, that amphibole phase cannot be monoclinic. These distinctions are critical to the correct identification of the amphiboles present.

**MAS's PLM Analysis**

**Refractive indices**

The measurement of refractive indices is accomplished by immersing the talcum powder in liquids with known refractive index. Using the light as it interacts at the boundaries of the grain and the liquid, one can measure by comparison the refractive index of the unknown particle in question. The refractive indices of a given material can be modeled as a function of both the composition and density of that material. A good example of this relationship is seen in the ability to distinguish between the amphibole minerals tremolite ($Ca_2Mg_5Si_8O_{22}(OH)_2$) and actinolite ($Ca_2(Mg,Fe)_5Si_8O_{22}(OH)_2$); this is due to the replacement of magnesium (Mg) for iron (Fe) which increases the refractive indices of actinolite compared to tremolite, likewise as Fe replaces Mg the density increases. Thus, in combination with the other required measurements the refractive index is an indirect measurement of chemical composition. In fact, one can by inference determine the composition of an amphibole group mineral by accurate measurement of the refractive indices (Troger 1979).

The measurement of the refractive index as performed by analysts at MAS was done using the technique: central stop dispersion staining. It is beyond the scope of this report to expound the physics of this technique. However, it is necessary for lay readers to understand the relationship of the colors observed by this technique and their relationship to the refractive index of a mineral relative to the refractive index of the immersing liquid. Figure 1 is adapted from Su 1998. It illustrates the different colors observed as a function of the matching wavelength between the refractive index of an unknown particle and the known refractive index of the liquid. Additional photographs have been added to the graph to better illustrate the colors seen with associated wavelength of match. Based on the wavelength of match exhibited by the color observed, one can measure the refractive index of the unknown when the refractive index of the liquid is near the refractive index of the unknown.

Based on the images presented in the MAS reports, there are two general comments that can be made regarding Dr. Longo's measurement of refractive index: 1) for some particles identified as tremolite the observed PLM images in dispersion staining are consistent with the refractive indices for tremolite. Figure 2 is an example of this, where the observed colors both parallel and perpendicular to the elongated particle are consistent with a low Fe monoclinic amphibole, i.e. consistent with tremolite; and 2) for the particle types identified as anthophyllite, and many of those identified as tremolite, the refractive indices are much too high relative to the refractive index of the oil which is 1.605. Figure 3 and Figure 4 are examples of these errors in the measurement. Based on the colors observed it is not possible to estimate the refractive index other than they are much higher than 1.605. Due to this fact, the composition of these observed amphiboles is much richer in Fe than the particle shown in Figure 2. However, when one compares the reported refractive indices for what MAS identifies as tremolite and anthophyllite, many of the reported anthophyllite and tremolite/actinolite particles do not exhibit the dispersion staining colors that would correlate with the reported measured refractive indices.

The images with the measured refractive indices also demonstrate that the laboratory failed to follow established practices for determining the refractive indices of the suspected amphibole minerals in question.

When the refractive index of the fiber is much greater than the refractive index of the liquid (the dispersion curves of both liquid and solid do not intersect in the visible spectrum), the dispersion staining color exhibited is white (ISO 22262-1, 7.2.3.7.6). Also, when the refractive index of the fiber is much lower than the liquid, the dispersion staining color exhibited is white. Therefore, it is critical that to accurately interpret dispersion staining colors for the purpose of refractive index determination, the known index of the liquid used must be reasonably close to matching the particle in question. In a textbook by Bloss (1999), Ch. 13, Dr. Su-Chun Su presents clear instructions on how to accurately determine the refractive indices of the minerals tremolite, actinolite, and anthophyllite. It is not possible to determine the refractive indices of tremolite, actinolite or anthophyllite using only a single refractive index liquid.

*"… measurements of the $\gamma$ and $\alpha$ indices of tremolite asbestos requires immersion in liquids 1.635 and 1.605 and use of Table 13-6. Similarly, determination of $\gamma$ and $\alpha$ for actinolite and anthophyllite fibers will require their immersion in liquids 1.640 and 1.615 …"* page 205.

The use of only 1.605 RI liquid also goes against ISO 22262-1 which states that for the "identification of tremolite, actinolite, and anthophyllite" RI liquids with "values of 1.605 and 1.630" should be used. And talc samples should be examined in 1.615 RI liquid and if there are no particles with $\gamma$ values higher than 1.615, then the fibers/structures should be classified as talc (ISO 22262-1 7.2.3.7.6).

The only refractive index liquid used by MAS has a value of 1.605. Given this fact, as well as the dispersion staining images included in its report, it is not possible to determine the refractive indices of many of the particles observed. Despite this impossibility, Dr. Longo continually records measurement of refractive index values that are impossible based on the PLM back-up data provided in his reports.

In fact, our own analysis of the same samples and the amphibole minerals observed therein indicates the observed refractive indices of the particles are much greater than can be measured in 1.605 refractive index liquid. The composition of these particles with higher refractive index, as determined by SEM-EDS, as well as the crystal structure of the particles, as determined by TEM-SAED and SEM-EBSD, indicate they are primarily the monoclinic amphibole cummingtonite with appreciable iron. Trace amounts of the biopyribole minerals, talc, clinojimthompsonite, and jimthompsonite have also been observed in our analyses to date. The refractive indices of cummingtonite and clinojimthompsonite (or other pyribole observed) overlap, and in addition the extinction angle for clinojimthompsonite is much less than that of cummingtonite and typical monoclinic amphiboles (Veblen and Burnham 1978 and Droop 1994), therefore making a positive identification with PLM alone very challenging, if not impossible.

Based on the images presented in the MAS reports, several instances of talc and amphibole intergrowths are clear, but not reported. A few instances are observed and explained, but several others exist. These particle types should in no way be considered asbestos as they are not defined as such.

Another nuance associated with these types of particles is the consistent misidentification of anthophyllite in the presence of tremolite based on the observation of parallel extinction. In fact, both the identification of tremolite and anthophyllite is incorrect in these samples where the refractive indices are much greater than 1.605. The amphibole being observed is monoclinic lying in different orientations resulting in different extinction characteristics. The orientation of the amphibole when it is attached and intergrown with the talc plates is such that the crystal will exhibit parallel extinction. This is because the (100) monoclinic amphibole plane is parallel with the (001) talc plane. This principle is discussed by Verkouteren and Wylie 2002, and Brown and Gunter 2003. This apparent parallel extinction could further be caused by the presence of clinojimthompsonite, as it has a much lower extinction angle than the monoclinic amphibole and will thus decrease the observed extinction angle. Thus, in the presence of a monoclinic amphibole and the evidence of the amphibole to biopyribole reaction, without the additional manipulation of the crystals it is not possible to determine if the amphibole is orthorhombic or monoclinic based on extinction properties from single particles if they have not been rotated perpendicular to the elongation. Figure 5 illustrates one such particle in RJLG sample number 315416 which corresponds to the MAS sample M69042-001, wherein MAS reports the presence of both tremolite and anthophyllite by PLM. As demonstrated in Figure 5 the particle is rolled under the microscope slide, such that a particle initially exhibiting parallel extinction as shown in C, changes to show inclined extinction in D. Furthermore, work performed by RJLG on specific particles that initially showed parallel extinction, when removed and either electron back-scatter diffraction or zone axis electron diffraction was performed, these crystals were cummingtonite, a monoclinic amphibole, or in a few instances clinojimthompsonite, a monoclinic biopyribole.

**PLM Morphology**

Despite the consistent misidentification of the type of amphiboles observed especially in samples derived from the Vermont talc deposits, the most important error made by MAS by PLM is the failure to determine if the particles being observed are in fact amphibole asbestos. In fact, the reporting of amphibole "asbestos" by MAS disregards the definitions and descriptions of asbestos in the ISO method that they cite as the method used. Their results ignore the very ISO definition of asbestos:

*"term applied to a group of silicate minerals belonging to the serpentine and amphibole groups which have crystallized in the asbestiform habit, causing them to be easily separated into long, thin, flexible, strong fibres when crushed or processed."*

ISO defines the asbestiform morphology as:

*"a) the presence of fibre aspect ratios in the range of 20:1 or higher for fibres longer than 5 µm;*
*b) the capability of longitudinal splitting into very thin fibrils, generally less than 0,5 µm in width;*
*c) in addition, observation of any of the following characteristics for the fibre type under consideration provides additional confirmation that the fibres are asbestiform:*
*1) parallel fibres occurring in bundles,*
*2) fibre bundles displaying splayed ends,*
*3) fibres in the form of thin needles,*
*4) matted masses of individual fibres,*
*5) fibres showing curvature".*

Furthermore, Dr. Longo ignores the direction of ISO as it cautions analysts that when the minerals tremolite, actinolite, and anthophyllite are encountered one cannot assume that one is dealing with these minerals in the asbestiform habit.

*"…the amphiboles tremolite, actinolite, and richterite/winchite were not generally used in commerce, and their presence in a product is more likely a consequence of naturally occurring contamination of one or more of the major constituents. Accordingly, no assumption can be made as to whether the amphibole is asbestiform or non-asbestiform".*

It is through ignoring the very definitions of asbestos that any amount of asbestos is reported by Dr. Longo. Repeatedly in deposition testimony concerning the PLM analysis he states that if the amphibole particle is greater than 3:1 aspect ratio it is asbestiform and thus asbestos. This is demonstrably not true.

Dr. Longo repeatedly cites in his reports to a classic paper from Campbell et al. 1977 from the US Bureau of Mines regarding the observed morphology for his particles. In this paper Campbell and his colleagues compared aspect ratio distributions of both tremolite and tremolite asbestos. These frequency diagrams were determined using SEM for all lengths of particles observed and did not differentiate between bundles of amphibole asbestos and single crystals of amphibole or amphibole asbestos. The significance of these nuances will be discussed in more detail when dealing with Dr. Longo's TEM analyses. Figure 6 illustrates the mean aspect ratios observed by Campbell for both anthophyllite versus anthophyllite asbestos and tremolite versus tremolite asbestos. Note that both the prismatic anthophyllite and tremolite have mean aspect ratios approximately 3:1 with a significant portion in excess of 3:1. This means that a significant portion of the particles observed by Campbell and his colleagues would be classified as asbestos if the deviations to the standard methods followed by Dr. Longo were scientifically valid. Furthermore, Dr. Longo cites to OSHA to support his claim, however OSHA ID 191 defines a fiber as:

*"Fiber: A particle longer than or equal to 5 µm with a length to width ratio greater than or equal to 3:1. This may include cleavage fragments".*

Further they define an asbestos fiber as:

*"Asbestos Fiber: A fiber of asbestos meeting the criteria for a fiber".*

The ISO 22262 method defines a "fibre" as an "elongated particle which has parallel or stepped sides" and has an aspect ratio greater than 3:1. Thus both the OSHA and ISO definition of fiber apply to any particle observed and are not a definition of asbestos or asbestiform. Dr. Longo's confounding the term fiber with asbestiform will lead to false positive results wherever non-asbestos amphiboles are present or other minerals, such as amphibole-talc intergrowths, are observed.

Dr. Longo has also sworn in deposition that the particles that MAS observed by PLM are "bundles", thus attempting to explain away the low aspect ratios observed. However, this again is demonstrably not true. The appearance of bundles of amphibole asbestos are distinct when compared to fragments of amphibole and based on the size and scale of the particles will be more readily observed (see Appendix C). Figures 2, 3, and 4 further illustrate the morphological differences of both standard tremolite asbestos and anthophyllite asbestos as provided in the ISO 22262-1 method and contrasted to the morphology of the particles observed by Dr. Longo in sample M69503-026. Note on the reference images the fibrillar growth habit (composed of fibers) nature of the particles; these are bundles. Note the complete lack of the fibrillar structure in the observed particles by Dr. Longo. In review of each of the produced particles' PLM images, none of them exhibit any asbestiform or bundle characteristics. When the data is treated on a sample by sample basis, none of the provided images document the presence of amphibole asbestos in any reported sample to date.

Appendix A contains each of the PLM Dispersion staining images produced by MAS and compares both the central stop dispersion colors exhibited, and morphology of the particles reported as anthophyllite to the reference images for anthophyllite asbestos found within ISO 22262-1.

Appendix B contains each of the PLM Dispersion staining images produced by MAS and compares both the central stop dispersion colors exhibited, and morphology of the particles reported as tremolite to the reference images for tremolite asbestos found within ISO 22262-1.

**Transmission Electron Microscopy**

Unlike polarized light microscopy, the TEM allows for direct measurements of both the chemical composition of a discrete particle through the use of energy dispersive spectroscopy techniques and determination of limited crystal structure information through election diffraction techniques. As both PLM and TEM are microscopes this allows for the direct observation of the general shape of the discrete particles. However, unlike PLM, the determination of the occurrence of bundles and other distinguishing features of asbestiform minerals (minerals crystallized in the asbestiform habit) is less straight forward due to the high magnification and necessarily small particle sizes that can be analyzed by TEM. Most amphibole asbestos particles

observable under the TEM are at the sub-bundle scale. Furthermore, unlike PLM, there is no way to rapidly screen particles, such as by refractive index, to analyze large amounts of material both quickly and reliably. By TEM, any elongated particle must be evaluated by SAED and/or EDS before the analysis can continue.

The use of EDS is critical in order to identify the specific amphibole species. As stated above most amphiboles are monoclinic and they have very similar crystal structures. Thus, the observation and indexing of zone axis diffraction patterns will not be substantively different between tremolite and actinolite, or tremolite and cummingtonite. However, these three amphiboles will each have unique chemical composition and once the monoclinic amphibole crystal structure is confirmed by diffraction techniques they can be reliably identified.

Electron diffraction techniques are critical in these analyses as there is the possibility of encountering many minerals with compositions similar to one of the possible minerals that are defined as asbestos. A few examples are talc and anthophyllite, tremolite and diopside, cummingtonite and anthophyllite, and any biopyribole. See Table 1 for the compositional and crystal structure information of the minerals at issue in these samples. Because of so many possible confounding minerals in these talcum powder samples only the most rigorous electron diffraction techniques are acceptable for identification of unknown discrete particles. Of critical importance is the indexing of any particle with dominant cationic compositions of only magnesium, silicon, and iron (Mg, Si, and Fe). The differentiation of talc, anthophyllite, cummingtonite, and any biopyribole is only possible with quantitative zone axis indexing of low index zones. It should be noted that in most instances' particles must be manipulated through "tilting" of the specimen holder in the TEM to obtain zone axis diffraction patterns. For any given mineral the orientation of that mineral relative to the electron beam determines the diffraction pattern observed.

A zone axis diffraction pattern is described in ISO 22262-1 as:

*"…. only those ED patterns obtained when the fibre is oriented with a principal crystallographic axis closely parallel to the incident electron-beam direction can be interpreted quantitatively. This type of ED pattern shall be referred to as a zone-axis ED pattern. In order to interpret a zone-axis ED pattern quantitatively, it shall be recorded photographically and its consistency with known mineral structures shall be checked".*

Principle crystallographic axes are those labeled a, b, and c as shown in Table 1, or a combination of each, for the minerals in question. Note that the measurement of 5.3 Å (in bold font) is not unique to any of the minerals in Table 1. Thus, the use of 5.3 Å spacings has little, if any, identification value in an unknown environment.

**MAS's TEM Analysis**

MAS cites to ISO 22262-2 for the use of TEM to analyze talc for asbestos. This method provides detailed information on how to prepare and analyze materials for asbestos and provide quantification on a mass basis. No part of the method provides for the calculation of asbestos content on a number of fibers per mass basis.

ISO 22262-2 requires an analyst to evaluate the particle's SAED pattern to determine information about the crystal structure for particles suspected to be amphibole (ISO 10312, pp. 39). It states:

*"…0.53 nm layer spacing of the random orientation ED pattern is not by itself diagnostic for amphibole."*

However, despite these clear statements, MAS employed the row-spacing technique to identify 113 amphibole structures in the MDL samples.

Specific to zone axis analysis, a total of 33 patterns were reportedly indexed using a zone axis pattern, and of these, only 5 were from the structures MAS claims to be anthophyllite, while the remaining 28 were tremolite diffraction patterns. If the methodology described in ISO 22262-2 (and ISO 10312) was followed, at least one SAED pattern from each suspected amphibole per sample must be confirmed using zone-axis methods. Furthermore, given the critical role electron diffraction plays in differentiated minerals with similar compositions, quantitative zone axis analysis efforts should have been focused on the Mg, Si, and Fe bearing particles where misidentification is most likely to occur.

ISO further states that an analyst must confirm amphibole from an unknown source by "obtaining recorded data which indicates exclusively the presence of amphiboles for fibers classified in the AZQ, AZZ, or AZZQ categories." The acronyms AZQ, AZZ and AZZQ are defined in ISO standard 10312 (and others). They represent a high "level" of analysis in which the "A" stands for amphibole, "Z" stands for quantitative zone axis SAED (meaning measured and indexed) and the "Q" represents quantitative EDXA. Thus for the AZZQ category, a specific particle must have two indexed zone axis patterns and compositions determined by EDS techniques in order to identify the unknown particle as amphibole. There is no evidence that MAS performed dual quantitative zone axis analysis or EDXA analysis, thus MAS cannot have satisfied the requirements of AZQ or AZZQ per sample that is required to confirm the mineral amphibole(s).

MAS observed and reported a total of 157 amphibole structures in its analysis of the MDL samples. For each of these observed amphiboles MAS attempted to provide at least one diffraction pattern and recorded and produced a total of 248 diffraction patterns. However, the vast majority of these patterns are not zone axis diffraction patterns or near zone axis patterns as required by ISO.

MAS also produced numerous talc diffraction patterns oriented approximately parallel to the [001] zone axis. Using the talc patterns as a basis of calibration, coupled with the ratios of the lattice spacings observed in the diffraction patterns, each of these diffraction patterns was reviewed and, when possible, indexed by using a combination of Dr. Shu-Chun Su's diffraction tables available to all NVLAP accredited laboratories for asbestos analysis, the electron diffraction software SingleCrystal,© and the use of mineral reference structures[1]. MAS failed to obtain measurable zone axis patterns for the majority of the particles and failed to index the few zone axis patterns that were collected correctly.

Of the 248 collected diffraction patterns, 92 of them could not be measured because they were not zone axis patterns or the images provided were of too poor quality and no lattice spacings could be determined. For the 248 collected diffraction pattern images, MAS determined 163 to be anthophyllite, 81 to be tremolite, and 4 to be anthophyllite-talc intergrowths. Of the 163 anthophyllite patterns, 55 were incorrectly identified as anthophyllite and are actually consistent with the monoclinic amphibole cummingtonite. 80 of the 81 tremolites were tremolite, and of the four anthophyllite talc intergrowths, none were identified correctly.

Figure 7a shows the image, EDS, and SAED with indexing solution [302] anthophyllite provided by MAS. Dr. Longo however failed to account for the space group extinctions that would be present in the orthorhombic Pnma space group. Figure 7b illustrates that the correct index of the observed diffraction pattern is the [301] monoclinic amphibole cummingtonite. Note the 18.1Å repeats in the non-zero layer lines for the anthophyllite pattern are not present in the observed pattern. Thus, the failure of proper diffraction pattern analysis as described in ISO 22262-2 misidentified the mineral present in this sample.

Dr. Longo also observed 4 particles that he identified as "transitional" structures. One of these patterns was able to be verified as an anthophyllite-talc transitional structure through indexing techniques, while the other three were indexed as much more complex biopyribole or a combination of talc, amphibole, and triple-chain silicates. An example of the latter is illustrated in Figures 8a and 8b from sample 20180061-65D where MAS misidentified anthophyllite and talc transitional. The correct indexing of this particle is talc and clinojimthompsonite. There is not an amphibole component.

In addition to these 4 structures, 13 of the structures MAS determined to be anthophyllite were indexed by RJLG as a biopyribole and intergrowths of talc, amphibole and biopyribole. One such example is illustrated in Figures 9a and 9b. Figure 9a includes the image, EDS, and two SAED patterns from sample M69042-008. The correct index of this particle is shown in Figure 9b; the two diffraction patterns index to [302] and [100] clinojimthompsonite. Thus, failure to measure

[1] The specific crystal structures used to evaluate Dr. Longo's electron diffraction patterns in this report are cited in the reference section and are taken from the peer reviewed literature.

and index the observed patterns resulted in a non-amphibole being mis-identified as anthophyllite.

Specific identification errors are as follows: one structure was indexed as an intergrowth of anthophyllite and talc however it is cummingtonite and talc, see Figure 10a and Figure 10b. Four structures identified as anthophyllite by Dr. Longo were observed as intergrowths of cummingtonite and talc, an example of this error is shown in Figure 11a and Figure 11b. Two structures identified as anthophyllite were observed as clinojimthompsonite and talc. Seven structures were observed as clinojimthompsonite. Two structures were observed as talc and unknown amphibole. One structure was observed as cummingtonite and biopyribole intergrowth. Lastly, two structures were observed as intergrowths of talc, cummingtonite, and biopyribole.

One structure MAS determined to be tremolite was found by RJLG to be clinopyroxene upon indexing. Figure 12a provides the image, EDS, and SAED pattern observed. Figure 12b provides the zone axis solution for this particle. The measurement of 6.6Å is diagnostic of clinopyroxene as this distance is not observed in tremolite.

Dr. Longo also failed to compare the measured SAED pattern to other possible minerals including talc. Two of the anthophyllite particles reported were determined by RJLG to be talc. On example is on page 571 of the November 2018 report from sample M68503-023-001 Diffraction1. MAS only verified this pattern as anthophyllite by measuring the row spacing of 5.22Å. RJLG measured $d_1$=4.74Å; $d_2$=4.51Å; $\beta$=62° and indexed as talc [001]. Because the diffraction data was not compared to other minerals, such as talc, the erroneous identification of anthophyllite resulted. Figure 13a and Figure 13b illustrate this mistake.

Appendix D contains all of the zone axis indexing that was possible based on the data provided by MAS.

**Morphology by TEM**

Dr. Longo and MAS reported a total of 184 structures, 169 of which are determined to be asbestos bundles and 15 are reported as asbestos fibers. This means that during the MAS TEM analysis, 92% of counted particles were classified as bundles.

Of the structures counted, 93, or 51%, were recorded as anthophyllite bundles while only 12 structures, or 7%, were recorded as anthophyllite fibers. Of the structures counted, 73, or 40%, were recorded as tremolite bundles while only 2% of were recorded as tremolite fibers.

To put these observations in context, the observation of “bundles” by TEM is a function of the size of observed particles. For amphibole type asbestos the mean diameter of the fibrils (fibers that are no longer divisible) are generally less than <0.5µm in diameter. This value will vary depending on the specific occurrence. The fiber width of asbestos fibrils is directly controlled to

formation conditions. Thus, where particles observed by TEM have widths < 0.5um, these are generally not bundles. Appendix C illustrates the of the observance of bundles as a function of magnification. Note that the magnifications and size ranges of particles observed by Dr. Longo generally occur at the sub-bundle level.

A bundle is a grouping of individual asbestos fibrils that only share the c-crystallographic axis. As such the diffraction patterns produced by bundles of asbestos fibrils are polycrystalline in nature, thus, if a particle is said to be a bundle, the resulting diffraction patterns will exhibit evidence of this.

To help illustrate the morphological appearance of a bundle, a TEM micrograph was obtained from the NIST SRM 1866 Amosite standard reference material and is shown in Figure 14a. Note the presence of "splayed" ends indicative of the separation of asbestos fibers from the bundle structure. The areas marked as A, B, and C in the lower image correspond to areas where zone axis diffraction patterns were obtained, and these are shown and discussed in Figures 14b, 14c, and 14d respectively. Area A illustrates the presence of multiple fibers sharing the c-axis of the fiber (elongation direction) but also shows characteristics of structurally incoherent polycrystalline material diagnostic of the fibrillar growth habit of asbestiform amphiboles. Area B zone axis diffraction pattern is shown in Figure 14c and lacks the presence of the incoherent polycrystalline nature of area A, however the presence of (100) twin plane is evident by the systematic weak reflections along the b* directions. The presence of nanometer-scale twinning is common in monoclinic amphibole asbestos fibers (Ring 1981). Finally, area C is shown in Figure 14d. The resulting zone axis diffraction pattern is as expected the combination of the polycrystalline fibrillar structure from area A and the (100) twin present in area B.

In review of the zone axis and near zone axis diffraction patterns collected by Dr. Longo there is no evidence of any of the particles exhibiting incoherent reflections consistent with those shown in Figure 14b and Figure 14d from the standard reference material. Therefore, none of his zone axis or near zone axis patterns demonstrate the occurrence of bundles of amphibole asbestos fibrils consistent with his use of the term.

Dr. Longo attempts to compare his TEM derived particle size distributions observed to those of Campbell et al. 1977. As discussed above these distribution frequencies were collected for all particle sizes regardless of aspect ratio and particle size by scanning electron microscopy at magnifications less than those used by conventional TEM. Compare this to the data collected by Dr. Longo which only focused on the greater than 5:1 aspect ratio portion of the distribution and focused by necessity on only the finest particle sizes. Therefore, since the particle size data were not collected in the same manner, one cannot compare the aspect ratio distributions derived by Campbell to those observed by Dr. Longo. To do so is comparing disparate data sets and such comparisons are scientifically and logically invalid.

In a recent publication by Van Orden et al. (2016) the aspect distributions with respect to particle widths were determined for specimens of amphiboles and the asbestiform varieties by field

emission SEM at magnifications comparable to standard TEM analysis. The amphibole asbestos specimens used were standard reference materials. When using the log aspect ratio distribution as a function of the log width, amphibole asbestos can be differentiated from non-asbestiform amphibole. The importance of this work as a means of comparison is critical as these data sets best match the data sets generated by Dr. Longo on the MDL samples during the TEM analysis in the peer reviewed literature. Furthermore, the data collection did not discriminate between individual fibers of asbestos and bundles of asbestos. Therefore, the potential subjective nature of this determination is not a factor in the discriminate analysis. Figure 15a illustrates these distributions for both actinolite and HSE actinolite asbestos. It is important to note that the type of amphibole and amphibole asbestos has no significant effect on the observed particle distributions. Figures 15b and 15c compare all of Dr. Longo's alleged anthophyllite asbestos and tremolite asbestos observed particles for all samples analyzed. The comparison of the population characteristics is consistent with the PLM morphological data that for both the alleged tremolite and anthophyllite particles, particles did not crystallize in the asbestiform habit.

Assuming that the above errors were not made in reviewing the concentrations of Johnson and Johnson talc based products (excluding Imerys MDL samples) the mean concentration reported is 23,623 f/g with standard deviation of 41,903. These values are derived using non-detects as half the sensitivity with n=49.

***Heavy Liquid Separation in analyzing Talc for asbestos.***

The use of heavy liquids to separate accessory minerals from talc was explored by Blount (1990, 1991) and a similar protocol is described in ISO22262-2. It should be noted that the use of density differences to separate mineral fractions is not a novel concept. It is also important to note that any separation or gravimetric reduction procedures is for preparation of the samples and does nothing to address the proper mineral identification procedures (as discussed above). MAS has implemented a modified protocol in several recent reports. However, given the information in the original work by Blount, the utility of this protocol for improving the sensitivity of PLM analysis for amphibole in a talc matrix is debatable. None of the MAS reports have demonstrated the efficiency of the separation technique to show that it actually provides a more sensitive method compared to simply examining a portion of the as received sample, as is done in standard testing methods such as ISO 22262-1 or EPA R-93/116.

The supporting information provided in Blount (1990) specific to her methodology indicates that a significant amount of any amphibole may actually be included with the talc portion that is removed via the heavy liquid separation using the Clerici liquid (a highly toxic water-soluble Thorium compound). Dr. Blount tested her method by adding a known quantity of the mineral dolomite, which has a similar density as amphibole, and measure the amount of dolomite in the separated material. The result of the test showed that in the best case, only 30% of the dolomite was recovered from the talc sample. This means that 70% of the mineral of interest, i.e. amphibole, that might be present in a sample is not recovered during the separation process and is lost. If chrysotile were present, 100% would be lost during the separation process.

When performing any gravimetric reduction technique to either improve detection or quantification of a given analyte one must assess whether and how the said methodology effects the analyte in question. Dr. Longo has failed to address two important disadvantages of a heavy liquid separation on talc recognized by Dr. Blount. The first of these is the failure to address chrysotile at all in the analysis for asbestos in these talcum powders. The second is the efficiency or the recovery of amphibole (if present at all) in the original material.

There are multiple factors that affect the ability of a given heavy liquid to effectively separate denser phases. Some of these are particle size, viscosity of the heavy liquid, and recovery methods of the sink fraction. Dr. Blount demonstrated that her recovery varied greatly depending on the method she used to recover the heavy fraction. Since Dr. Longo deviated from her method by using a different heavy liquid, different spin times, and different recovery method, the efficiency is simply unknown for his samples. Without knowing the efficiency of the separation, he cannot report quantitative data as the amount of material lost or not recovered is unknown. Furthermore, unknown for both Dr. Blount and Dr. Longo's data is the relative efficiency of their preparations on the fine particle sizes.

Given these two problems, it is prudent to examine the untreated sample to ensure that both chrysotile is analyzed for and that any amphibole is observed and what is observed is not biased in an unknown manner. The time spent analyzing a sample for asbestos by standard XRD, PLM, and TEM methodologies analyses for both chrysotile and amphibole mineral types, thus these are superior to the use of only heavy liquid followed by the PLM and TEM analysis described by MAS. The purported increased sensitivity achieved through heavy liquid separation is accompanied by an unknown loss of the minerals of interest due to the efficiency of the separation and therefore any claims of superior analytical sensitivity and quantitative data should be treated with caution. Lastly, the inability to analyze for chrysotile while preparing the samples with heavy liquids still requires that one must analyze the sample without any separation techniques to determine chrysotile content. Thus, one must still analyze the sample without heavy liquid separation techniques.

***Work performed by MAS to attempt to validate its methodology***

MAS has produced numerous studies in order to attempt to show validation or repeatability of its methodology. However, in each case the approach taken cannot be used to claim method validation. The errors described above are systematic errors that relate directly to the methodology chosen, specifically mineral identification and determination of the asbestiform habit. In order to validate a methodology, one must show that the method does not result in either false positives or false negatives, or at the least, the frequency of such events are within an acceptable error rate. Thus, their "validation" studies only show that MAS follows its chosen methodology, and does not answer the question whether its methodology provides accurate

results: the correct identification of minerals species and whether the minerals crystallized in the asbestiform habit.

Thus, in order to validate its methodology, MAS would have to demonstrate that its deviations from the standard methods described above produce at a minimum a consistent and/or superior result. For example, if a talc sample was spiked with known amounts of both tremolite asbestos and non-asbestos tremolite, does the methodology followed by MAS arrive at the correct result in both mineral identification and morphological habit? Since the stated methodology followed by MAS deviates from the generally accepted standard methodologies in both mineral identification procedures and the determination of the asbestiform habit, it cannot.

**Conclusions**

Dr. Longo's deviations from the standard testing methodologies he cites as the methodology MAS follows leads to consistent false positive test results for asbestos.

The primary errors made by PLM concern the measurement of refractive index, use of extinction angle, and failure to conduct discriminate analysis for the morphological habit of observed particles. In each case Dr. Longo deviates from the standard methodology he cites to have followed in the ISO2226-2 methods.

The primary errors made by TEM deal with the correct indexing of electron diffraction patterns of what MAS consistently misidentifies as anthophyllite. These particles are shown to be cummingtonite with various degrees of intergrowths of biopyribole due to the amphibole to talc reaction. Furthermore, Dr. Longo misidentifies particles as bundles when no such morphological features are present. In addition, all supporting data from SAED analysis contradict the presence of asbestiform bundles. Lastly, when the morphological data from MAS's PLM analysis is compared to the same data collected from established samples of asbestiform and non-asbestiform amphiboles, it is clear the MAS data is more consistent with a non-asbestiform population.

Finally, the discrepancies between the types of amphiboles observed by MAS using PLM and those observed by TEM, for the Vermont sourced samples, are readily resolved when the zone axis indexing and optical characterization is performed correctly. Most of the amphiboles identified as anthophyllite by MAS using TEM are in fact the mineral cummingtonite, with some of the amphibole reacting to form talc and other biopyribole phases (e.g. clinojimthompsonite). The PLM data reporting the monoclinic amphibole tremolite in these samples with high refractive index are in fact the monoclinic amphibole cummingtonite.

I reserve the right to amend this report as more information and data is made available to me.

Sincerely,

Matthew S. Sanchez, PhD
Principal Investigator
msanchez@rjleegroup.com
724 387-1947

Attachments

Appendix A – Anthophyllite PLM comparisons
Appendix B – Tremolite PLM comparisons
Appendix C – Bundle as a function of magnification
Appendix D – TEM SAED comparison MAS indexed to RJLG indexed
Appendix E – Bivariant Log Aspect Ratio vs. Log Width Distribution Plots

**References**

Blount, A.M. (1990) Detection and Quantification of Asbestos and Other Trace Minerals in Powdered Industrial-mineral Sample. Process Mineralogy. Vol.9, pp. 557-570.

Blount, A.M. (1991) Amphibole Content of Cosmetic and Pharmaceutical Talcs. Environmental Health Perspectives. Vol. 94, pp. 225-230.

Brown, B.M., and Gunter, M.E. (2003) Morphological and Optical Characterization of Amphiboles from Libby, Montana U.S.A. by Spindle Stage Assisted – Polarized Light Microscopy. The Microscope. Vol. 51, pp. 121-140.

Campbell, W.J., Blake, R.L., Brown, L.L., Cather, E.E., and Sjoberg, J.J. (1977) Selected Silicate Minerals and Their Asbestiform Varieties. Mineral Definitions and Identification-Characterization. United States Department of the Interior. Bureau of Mines Information Circular 8751.

Droop, T.T.R. (1994) Triple chain pyriboles in Lewisian Ultramafic Rocks. Mineralogical Magazine. Vol. 58, pp 1-20.

International Standard Organization Standard Method 22262-1: Air quality – Bulk materials – Part 1: Sampling and qualitative determination of asbestos in commercial bulk materials.

International Standard Organization Standard Method 22262-2: Air quality – Bulk materials – Part 2: Quantitative determination of asbestos by gravimetric and microscopy methods.

International Standard Organization Standard Method 22262-3: Air quality – Bulk materials – Part 3: Quantitative determination of asbestos by X-Ray diffraction method.

International Standard Organization Standard Method 10312: Air quality – Bulk materials – Determination of asbestos fibres – Direct-transfer transmission electron microscopy method.

McCrone, W.C. (1980) The Asbestos Particle Atlas. Ann Arbor Science Publishers, Inc. Ann Arbor Michigan.

Nesse W.D. (2000) Introduction to Mineralogy. Oxford University Press, Inc. 198 Madison Avenue, New York.

OSHA ID 191 (1992) Polarized Light Microscopy of Asbestos. Branch of Physical Measurements and Analysis. OSHA Salt Lake Technical Center.

Ring, S.J. (1981) Identification of Amphibole Asbestos Fibers, Including Asbestos, using Common Electron Diffraction Patterns. Chapter 9. Electron Microscopy and X-ray Applications to Environmental and Occupational Health Analysis, Vol. 2. Ann Arbor Science Publisher, Inc.

Su, S.C. (1998) Dispersion Staining: Principles, Analytical Relationships and Practical Applications to the Determination of Refractive Index. Microscope Vol. 46:3 pp. 123-146.

Troger, W.E. (1979) Optical Determination of Rock-Forming Minerals. Part 1. Determinative Tables English Edition of the Fourth German Edition. E. Schweizerbart/sche Verlagscuchhandlung (Nagele U. Obermiller) Stuttgart 1979.

Van Orden, D.R., Lee, R.J., Hefferan, S., Schlaegle, S., and Sanchez, M. (2016) Determination of the Size Distribution of Amphibole Asbestos and Amphibole Non-Asbestos Mineral Particles. The Microscope. Vol. 64, pp 13-25.

Veblen, D.R. and Burnham C.W. (1978) New biopyriboles from Chester, Vermont: I Descriptive Mineralogy. American Mineralogist. Vol. 63. pp. 1000-1009.

Veblen, D.R. and Burnham C.W. (1978) New biopyriboles from Chester, Vermont: II The crystal chemistry of jimthompsonite, clinojimthompsonite, and chesterite, and the amphibole-mica reaction. American Mineralogist. Vol. 63. pp. 1053-1073.

Verkouteren, J.R., and Wylie, A.G. (2002) Anomalous optical properties of fibrous tremolite, actinolite, and ferro-actinolite. American Mineralogist. Vol. 87, pp. 1090-1095.

**Crystal Structure References**

Sheet Silicates

Lizardite (serpentine) – Mellini, M., and Zanazzi, P.F. (1987) Crystal structures of Lizardite, 1T and lizardite-2H1 from Coli, Italy. American Mineralogist. Vol. 72, pp. 943-948.

Talc – Reviews in Mineralogy Vol. 18, p233. Mineralogical Society of America.

Pyroxene

Diopside – Gordon, W.A., Peacor, D.R., Brown, P.E., and Essene, E.J. (1981) Exsolution relationships in a clinopyroxene of average composition $Ca_{0.43}Mn_{0.69}Mg_{0.82}Si_2O_6$:X-ray diffraction and analytical electron microscopy. American Mineralogist, Vol. 66, pp. 127-141.

Amphiboles

Anthophyllite – Walitzi, E.M., Walter, F., Ettinger, K. Verfeinerung der Kristallstruktur von Anthophyllite vom Ochsenkogel/Gleinalpe, Oesterreich.

Actinolite – Evans, B.W. and Yang, H. (1998) Fe-Mg order-disorder in tremolite-actinolite-ferro-actinolite at ambient and high temperature Sample: NMNH 93728 from Greiner, Zillertal, Austria in act-talc rock. American Mineralogist Vol. 83. PP 458-475.

Cummingtonite – Yang, H. and Hirschmann, M.M. (1995) Crystal structure of *P2.1m* ferromagnesian amphibole and the role of cation ordering and composition in the *P2/m-C2/m* transition in cummingtonite. American Mineralogist Vol. 80, pp. 916-922.

Tremolite – Hawthorne, F.C. and Grundy, H.D. (1976) The Crystal Chemistry of the Amphiboles: IV. X-ray and Neutron Refinements of the Crystal Structure of Tremolite. Canadian Mineralogist. Vol. 14, pp. 334-345.

Biopyriboles

Jimthompsonite - Veblen, D.R. and Burnham C.W. (1978) New biopyriboles from Chester, Vermont: II The crystal chemistry of jimthompsonite, clinojimthompsonite, and chesterite, and the amphibole-mica reaction. American Mineralogist. Vol. 63. pp. 1053-1073.

Clinojimthompsonite - Veblen, D.R. and Burnham C.W. (1978) New biopyriboles from Chester, Vermont: II The crystal chemistry of jimthompsonite, clinojimthompsonite, and chesterite, and the amphibole-mica reaction. American Mineralogist. Vol. 63. pp. 1053-1073.

Chesterite- Veblen, D.R. and Burnham C.W. (1978) New biopyriboles from Chester, Vermont: II The crystal chemistry of jimthompsonite, clinojimthompsonite, and chesterite, and the amphibole-mica reaction. American Mineralogist. Vol. 63. pp. 1053-1073.

**Table 1.** Mineral name, composition, crystal system, space group, and crystal structure data for the minerals discussed in this report.

| Mineral | Composition | Crystal System | Space Group | a (Å) | b (Å) | c (Å) | β° |
|---|---|---|---|---|---|---|---|
| **Sheet Silicates** | --- | --- | --- | --- | --- | --- | --- |
| Serpentine | $Mg_3Si_2O_5(OH)_4$ | Monoclinic | C2/m | **5.3** | 9.25 | 7.3 | 93 |
| Talc | $Mg_3Si_4O_{10}(OH)_2$ | Triclinic | C-1 | **5.29** | 9.17 | 9.46 | 98.68 |
| **Pyroxene** | --- | --- | --- | --- | --- | --- | --- |
| Diopside | $CaMgSi_2O_6$ | Monoclinic | C2/c | 9.75 | 8.9 | **5.25** | 105.6 |
| **Amphiboles** | --- | --- | --- | --- | --- | --- | --- |
| Actinolite | $Ca_2(Mg,Fe)_5Si_8O_{22}(OH)_2$ | Monoclinic | C2/m | 9.85 | 18.1 | **5.3** | 105 |
| Anthophyllite | $(Mg,Fe)_7Si_8O_{22}(OH)_2$ | Orthorhombic | Pnma | 18.5 | 18.1 | **5.27** | 90 |
| Cummingtonite | $(Mg,Fe)_7Si_8O_{22}(OH)_2$ | Monoclinic | C2/m | 9.45 | 17.95 | **5.27** | 102 |
| Tremolite | $Ca_2Mg_5Si_8O_{22}(OH)_2$ | Monoclinic | C2/m | 9.85 | 18.1 | **5.3** | 105 |
| **Biopyriboles** | --- | --- | --- | --- | --- | --- | --- |
| Clinojimthompsonite | $(Mg,Fe)_{10}Si_{12}O_{32}(OH)_4$ | Monoclinic | C2/c | 9.86 | 27.2 | **5.3** | 109.5 |
| Jimthompsonite | $(Mg,Fe)_{10}Si_{12}O_{32}(OH)_4$ | Orthorhombic | Pbca | 18.6 | 27.2 | **5.3** | 90 |
| Chesterite | $(Mg,Fe)_{17}Si_{20}O_{54}(OH)_6$ | Orthorhombic | A2ma | 18.6 | 45.3 | **5.3** | 90 |

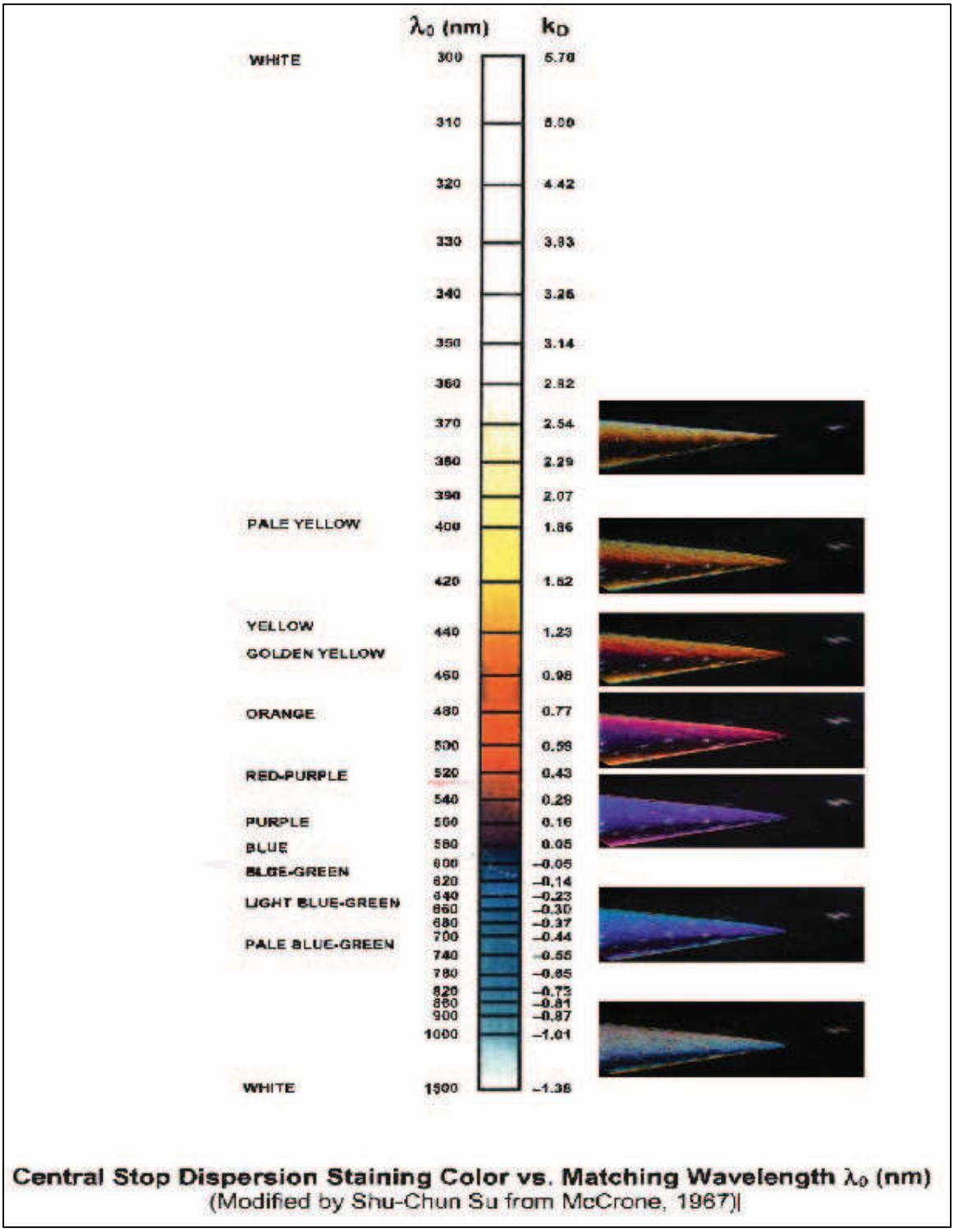


**Figure 1.** Example of observed color by dispersion staining as a function of wavelength of match in the visible spectrum. The images on the right are added photographs at wavelengths to better illustrate the observed colors. Where there is a near match for $\lambda_{(d)}$ the color is described as red-purple.

Figure D.37 — HSE tremolite in 1,605 RI liquid viewed in dispersion staining — Fibre lengths parallel to polarizer vibration direction

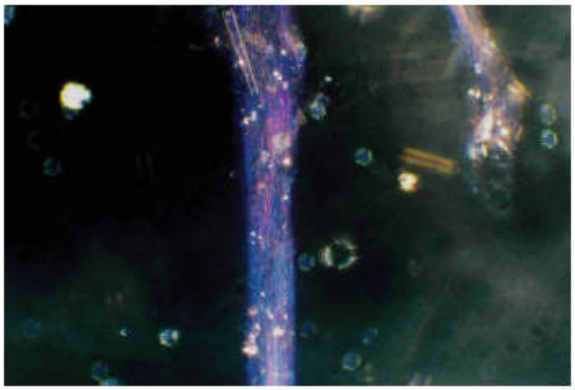

Figure D.38 — HSE tremolite in 1,605 RI liquid viewed in dispersion staining — Fibre lengths normal to polarizer vibration direction

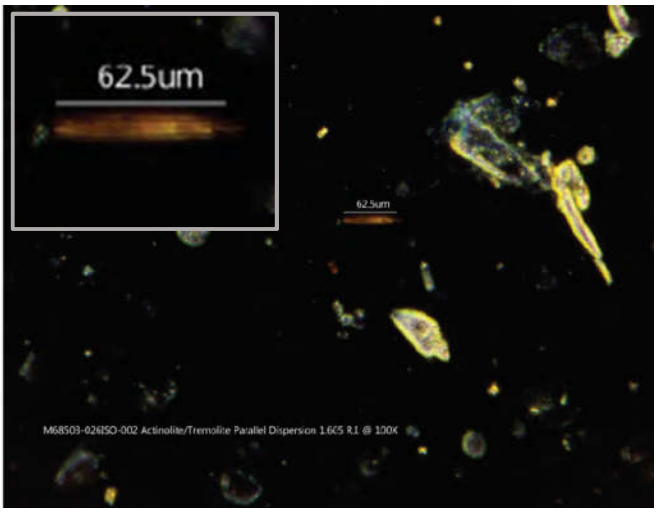


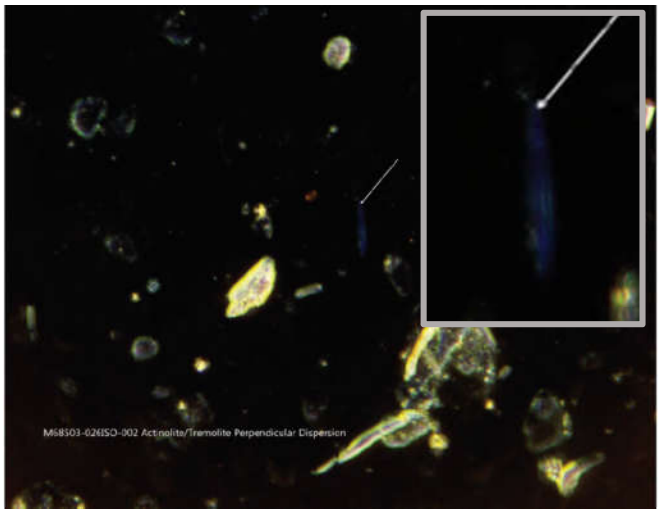


**Figure 2.** Comparison of reference tremolite asbestos to MAS PLM images. *Top:* Figures D.37 and D.38 from ISO 22262-1 illustrating reference HSE tremolite asbestos in 1.605 oil displaying dispersion staining colors of yellow in parallel and blue-purple in perpendicular. *Bottom:* Images from sample M69503-026 a particle in 1.605 oil displaying the correct dispersion staining color for the RI of tremolite that MAS recorded. Also, note the morphology of the particle is not similar as the HSE tremolite asbestos exhibits the asbestiform habit and is made of bundles composed of thin fibers while the particle in MAS's images is blocky and a single crystal, and thus not asbestiform.

Figure D.37 — HSE tremolite in 1,605 RI liquid viewed in dispersion staining — Fibre lengths parallel to polarizer vibration direction

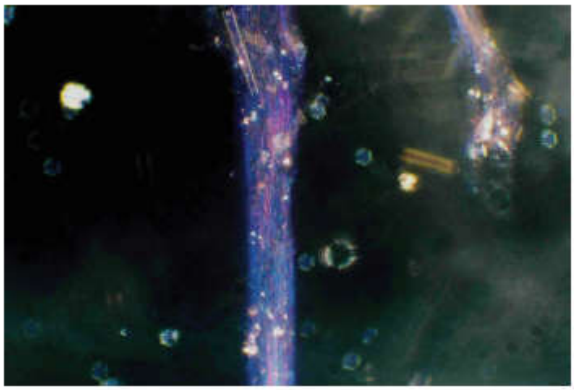

Figure D.38 — HSE tremolite in 1,605 RI liquid viewed in dispersion staining — Fibre lengths normal to polarizer vibration direction

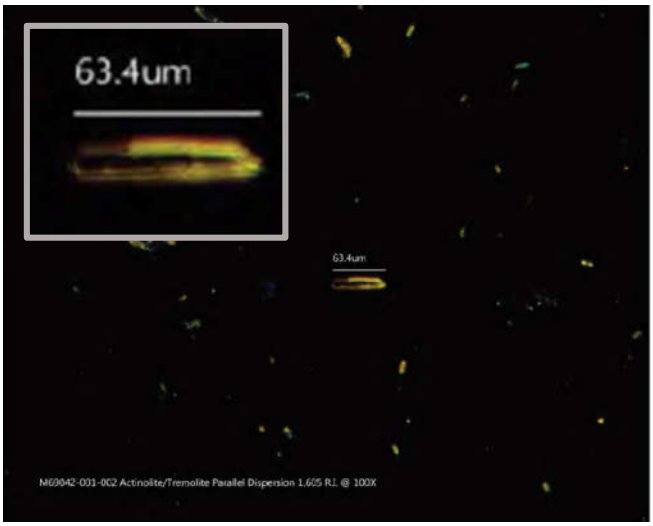


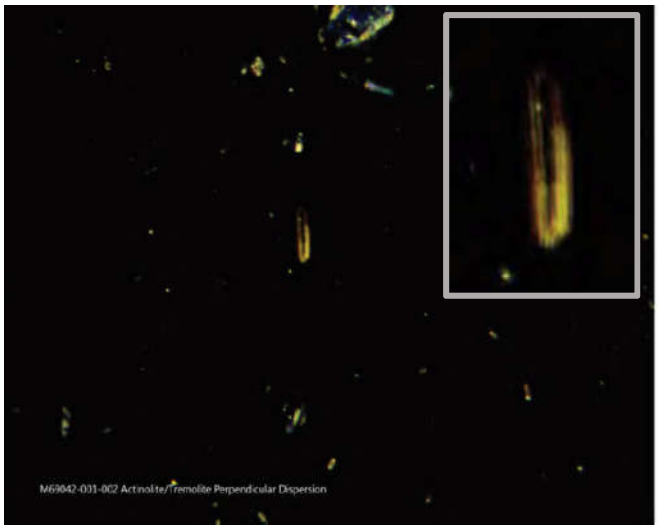


**Figure 3.** Comparison of reference tremolite asbestos to MAS PLM images. *Top:* Figures D.37 and D.38 from ISO 22262-1 illustrating reference HSE tremolite asbestos in 1.605 oil displaying dispersion staining colors of yellow in parallel and blue-purple in perpendicular. *Bottom:* Images from sample M69042-001 of a particle displaying the incorrect dispersion staining colors for the RI of tremolite that MAS recorded. Also, note the morphology of the particle is not consistent as the HSE tremolite asbestos exhibits the asbestiform habit and is made of bundles composed of thin fibers, while the particle in MAS's images is blocky and a single crystal, and thus not asbestiform.

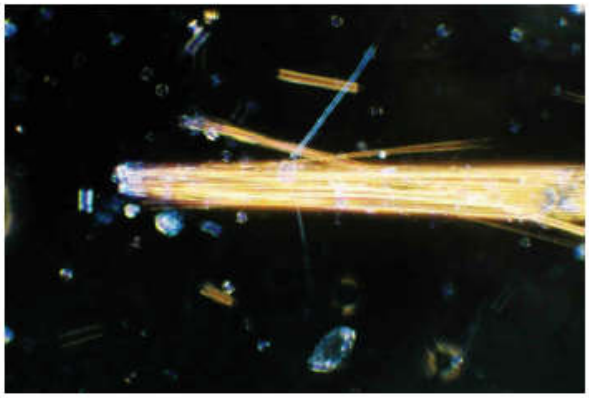

Figure D.47 — HSE anthophyllite in 1,605 RI liquid viewed in dispersion staining — Fibre lengths parallel to polarizer vibration direction

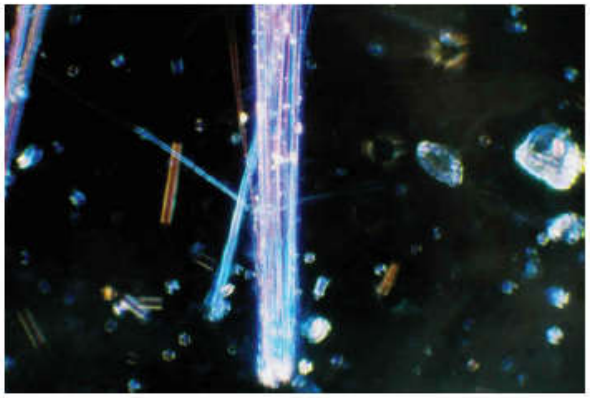

Figure D.48 — HSE anthophyllite in 1,605 RI liquid viewed in dispersion staining — Fibre lengths normal to polarizer vibration direction

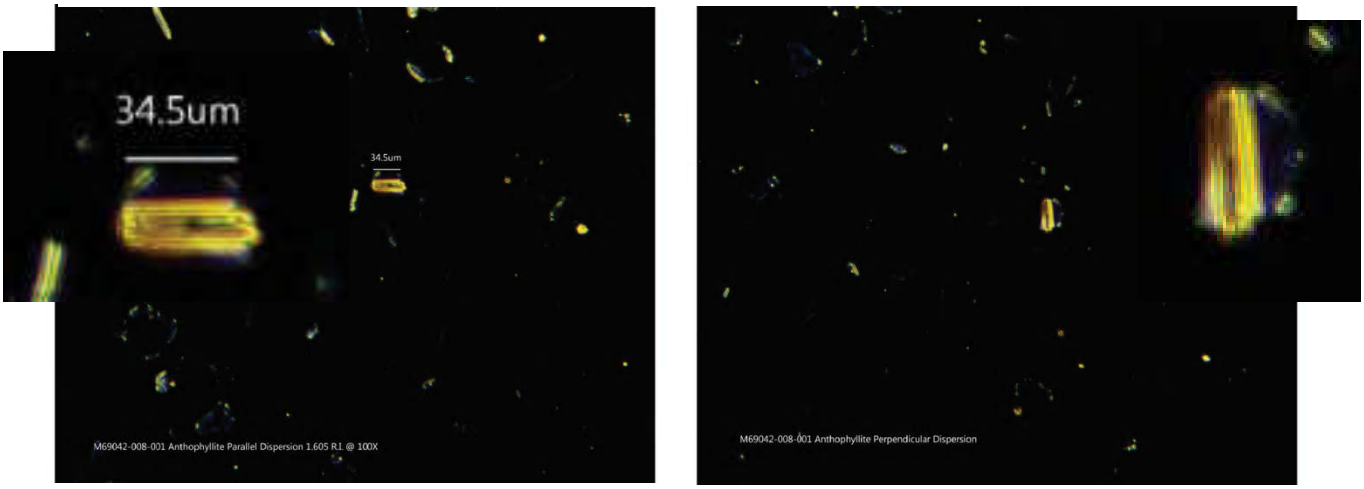


**Figure 4.** Images comparing dispersion staining colors from ISO 22262-1 and MAS images from sample M69042-008-001. *Top:* Figures D.47 and D.48 from ISO 22262-1 showing reference HSE anthophyllite asbestos in 1.605 oil. The parallel image in D.47 shows yellow-orange and the perpendicular image in D.48 shows purple blue colors. This is in direct contrast to Dr. Longo's images on the bottom which both display yellow-orange coloring. Also, note the morphology of the particle is not similar as the HSE anthophyllite asbestos exhibits the asbestiform habit and is made of bundles composed of thin fibers while the particle in MAS's images is blocky and a single crystal, and thus not asbestiform.

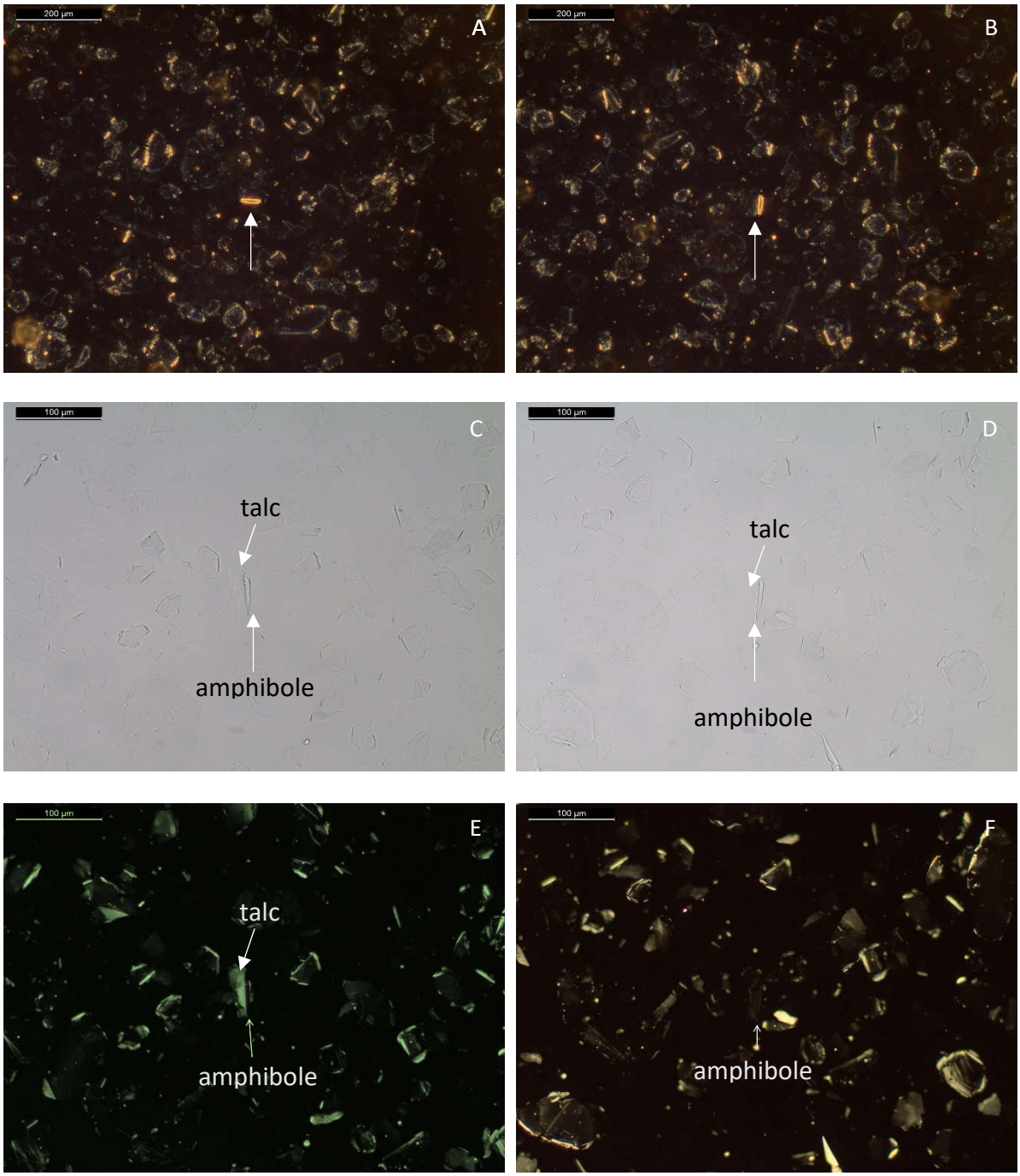


**Figure 5.** Amphibole talc intergrowth particle. A-B: dispersion staining images parallel and perpendicular demonstrating refractive index much higher than 1.605 immersion liquid. C-D: plane polarized light micrographs demonstrating parallel (C) and inclined (D) extinction positions. E-F: cross polarized light micrographs taken at same orientations as C & D demonstrating complete extinction of amphibole particle. The particle was manipulated to rotate the particle relative to the long dimension of the amphibole particle. Without performing this manipulation, the particle would have been confused with an orthorhombic phase when in fact it is a monoclinic phase as demonstrated by the presence of inclined extinction.

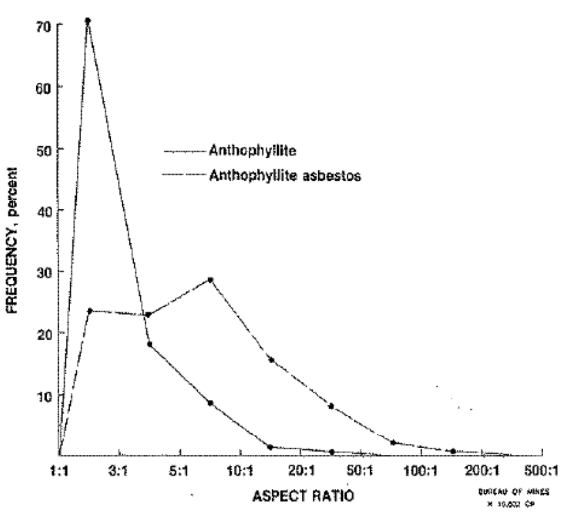


FIGURE 41. - Frequency polygons for the aspect ratios of anthophyllite and anthophyllite asbestos.

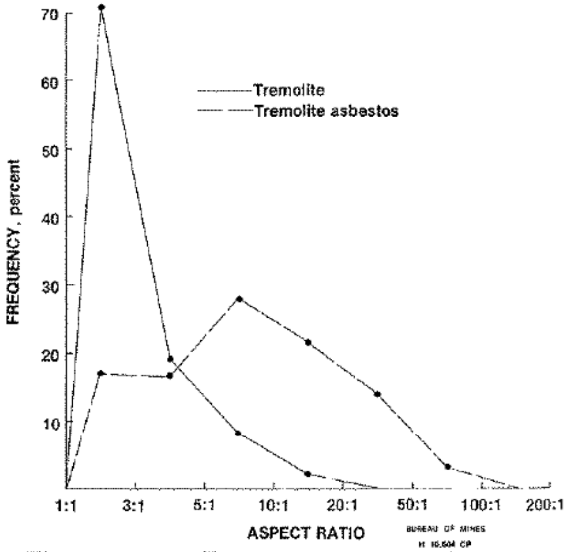


FIGURE 42. - Frequency polygons for the aspect ratios of tremolite and tremolite asbestos.

**Figure 6.** Frequency distributions of aspect ratios of anthophyllite vs. anthophyllite asbestos, and tremolite vs. tremolite asbestos taken from Campbell et al. 1977. Note that if a 3:1 aspect ratio is used then a significant portion of both the tremolite and anthophyllite would be erroneously classified as asbestos.

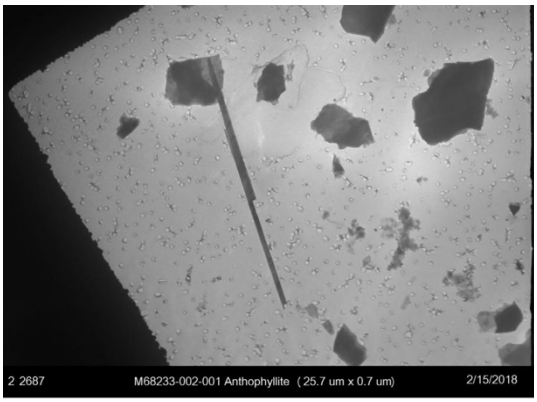


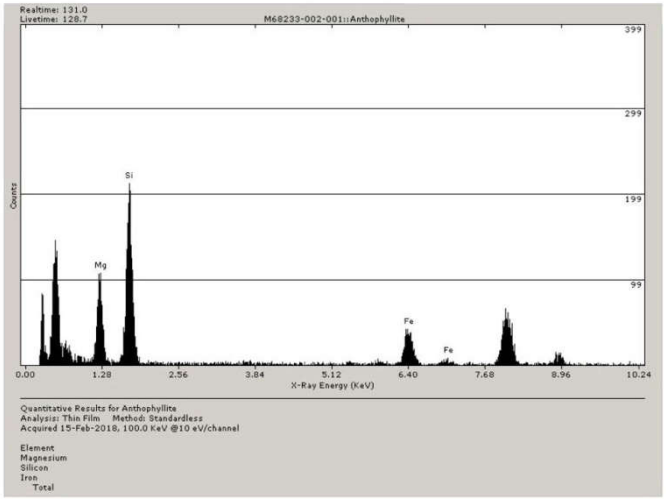


**VERIFICATION OF AMPHIBOLE DIFFRACTION PATTERN AT ZERO TILT**

| Camera K (pixelA) | Meas. Distance (pixels | Calculate Spacing (A) |
|---|---|---|
| 526.3 | See explanation | NA |

**Streaking Observed:** _ **Closely spaced dots:** _

**Type of amphibole diffraction verified:** Anthophyllite

**MAS Job #:** M68233-002-001 **Film #:** 2-2685

**Analyst:** Anthony Keeton **Date of Photo:** 2/15/2018

**Date Verified:** 2/15/2018 **EDS Verified:** Yes

**Unable to verify pattern:** _____

**Explanation:** d(hko) = 8.96; d(hkl) = 1.71; Angle = 85° ZA = [302]

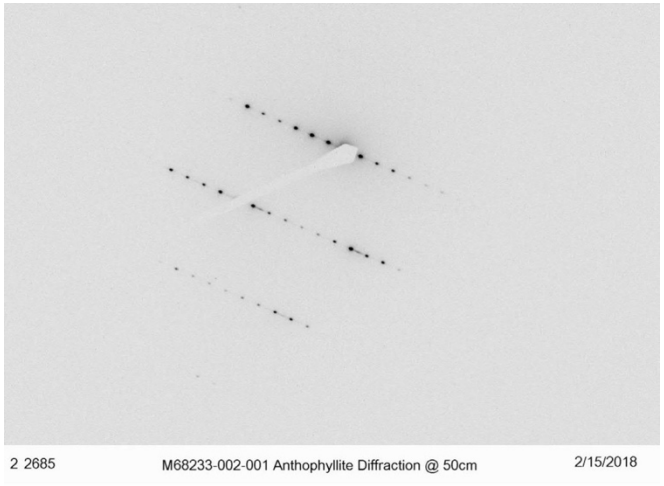


**Figure 7a.** Image, EDXA, and SAED from structure 001 from M68233-002 along with diffraction measurements. Dr. Longo misidentified the diffraction pattern as the [302] zone of anthophyllite.

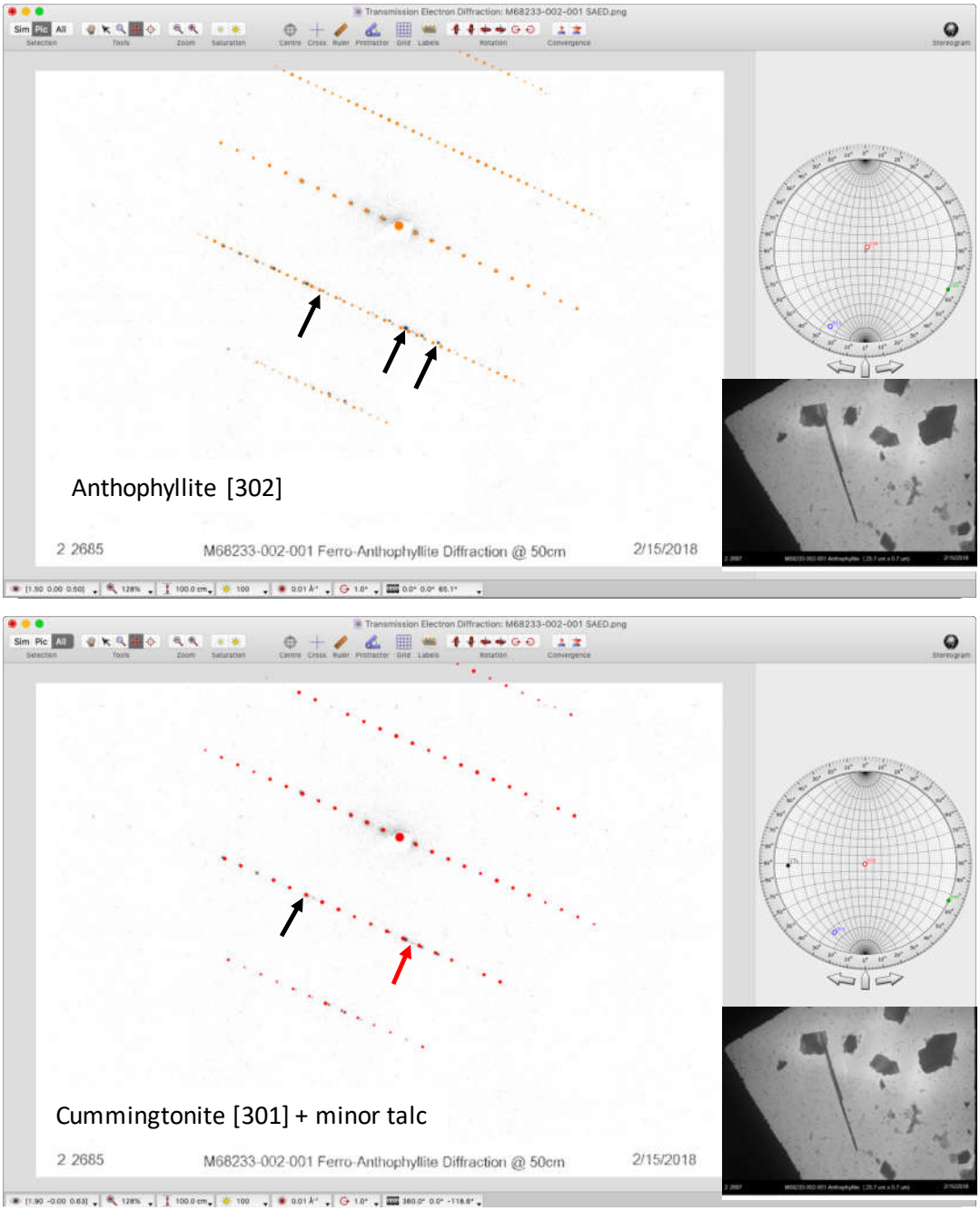


**Figure 7b.** Diffraction review from M68233-002-001. *Top:* Single Crystal simulation of the [302] anthophyllite zone (in orange) indexed by MAS overlaid onto the SAED image. If this zone was correct the non-zero layer lines would exhibit a 18.1Å spacing. The arrows indicate where the simulation does not overlay with the actual pattern. *Bottom*: RJLG index the same pattern as [301] Cummingtonite (in red) with minor talc intergrowths. The black arrow is showing that the spots overlay since the spacing is approximately 9.01Å while the red arrow is showing where coherent talc intergrowths are evident.

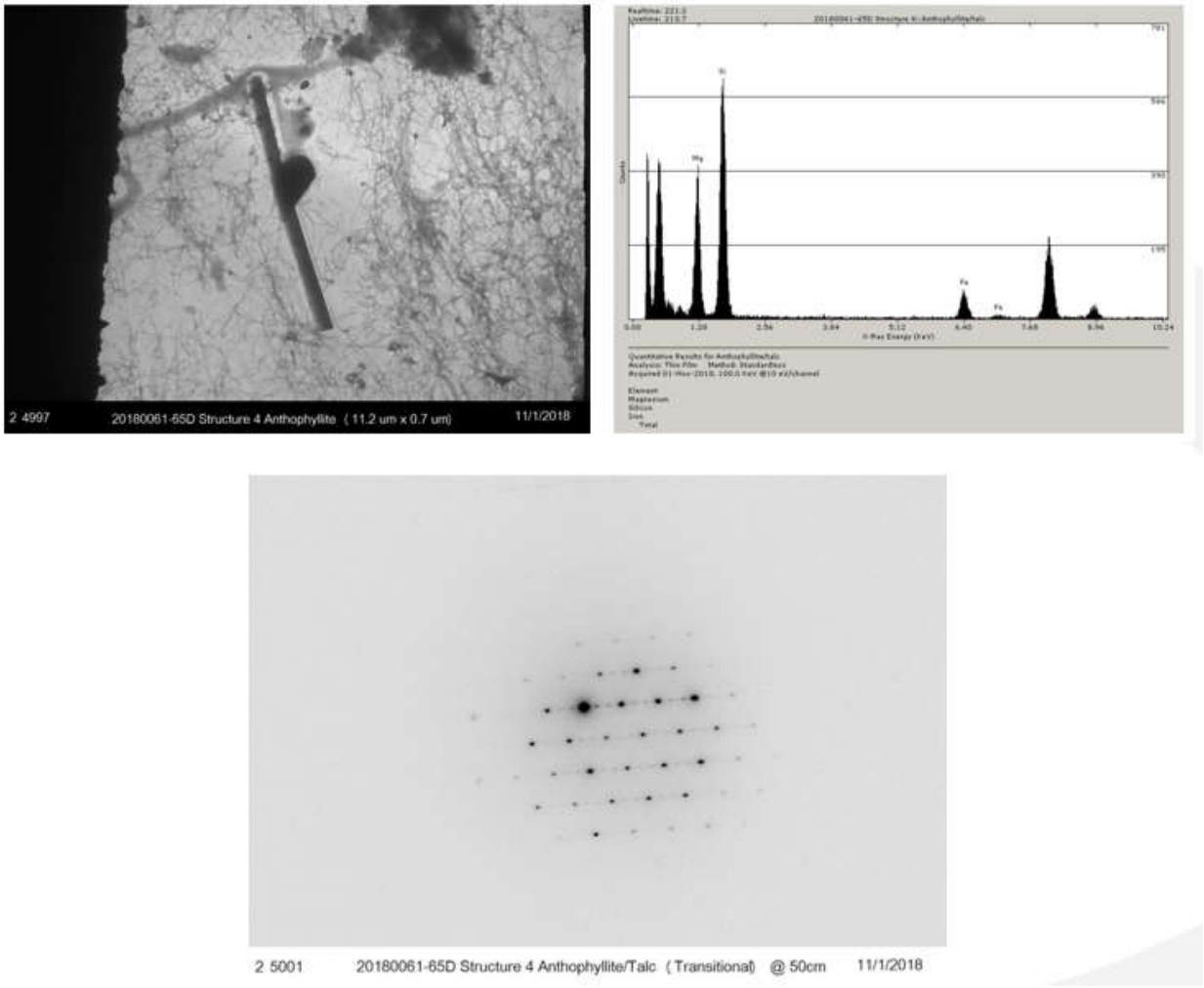


**Figure 8a.** Image, EDS, and SAED patterns from structure 4 from 20180061-65D. Dr. Longo misidentified as a transitional structure talc-anthophyllite.

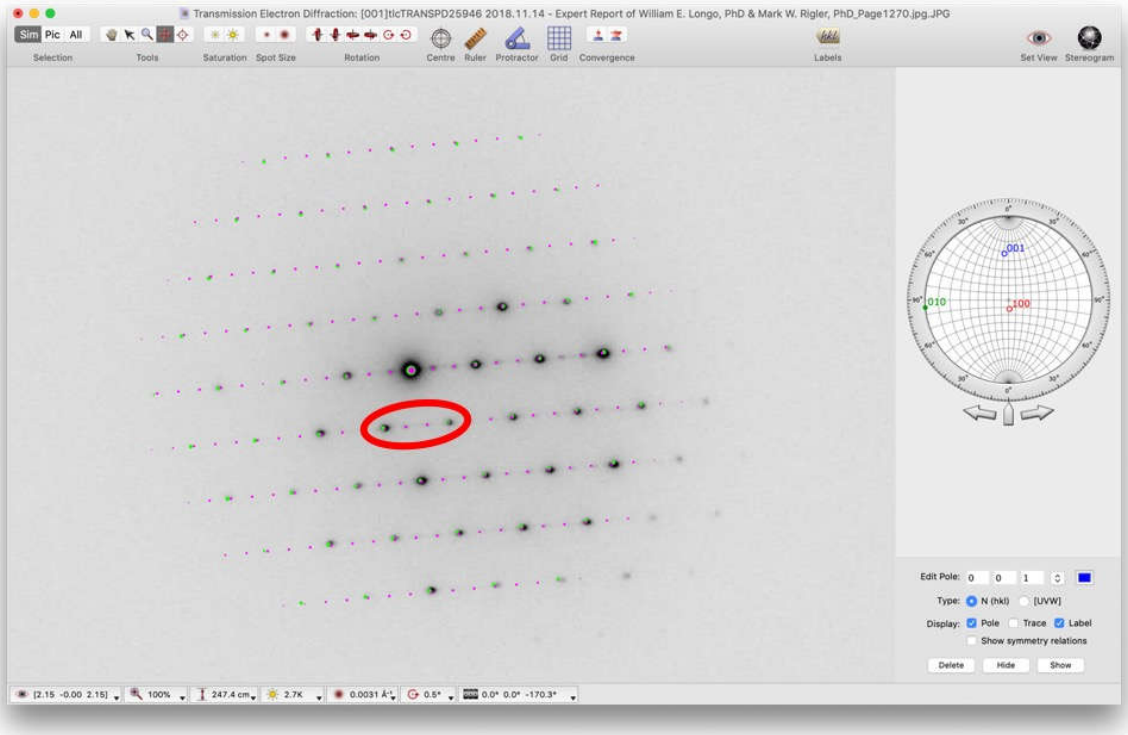


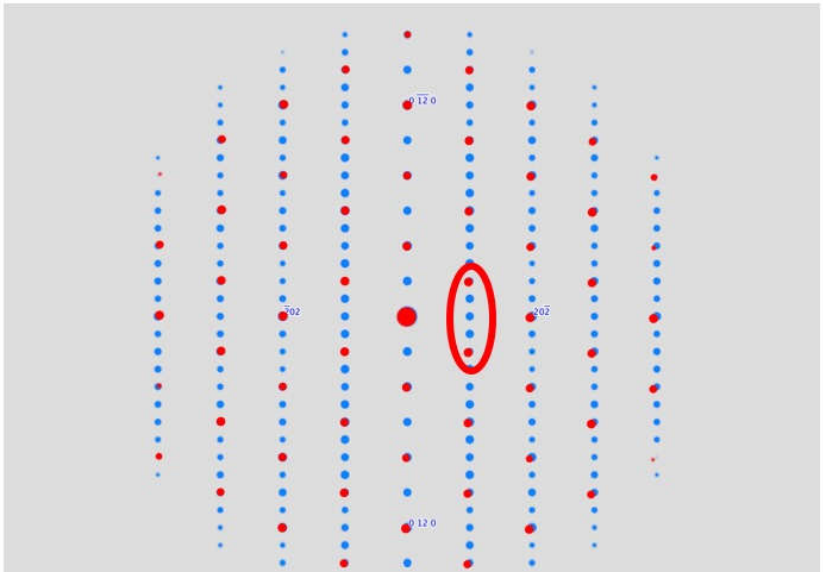


**Figure 8b.** Diffraction review of the SAED pattern from structure 4 of 20180061-65D. Pattern indexed using Single Crystal showing [001] talc (green) and [101] clinojimthompsonite (magenta). Bottom: Single Crystal simulation of Anthophyllite [101] with talc [001]. Notice the differences in the two patterns circled in red. If this was anthophyllite one would see three (3) reflections between the talc reflections in red, however on the observed pattern there are only two (2). This is consistent with a triple-chain monoclinic C lattice, thus clinojimthompsonite.

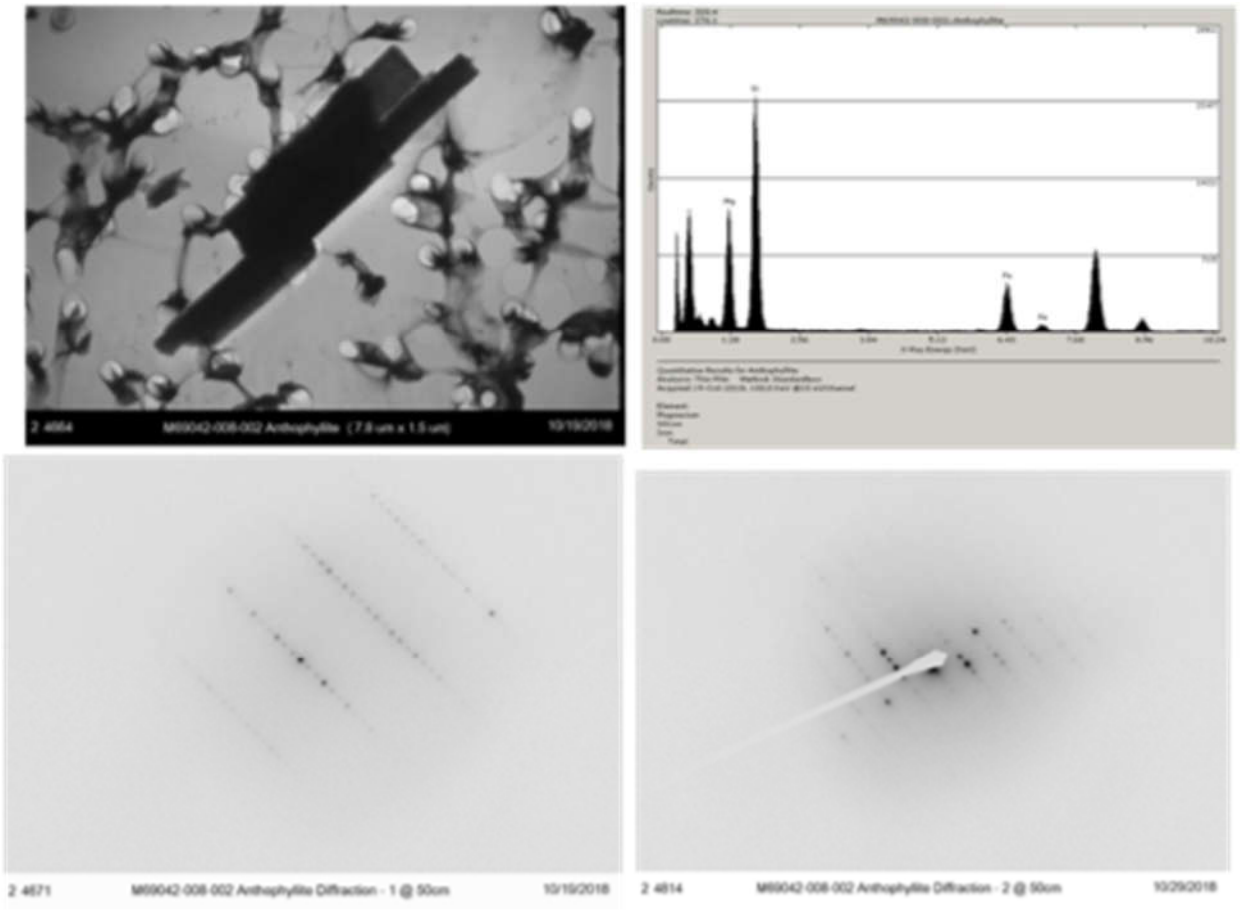

**Figure 9a.** Image, EDS, and two SAED patterns from structure 002 from M69042-008. Dr. Longo misidentified as anthophyllite.

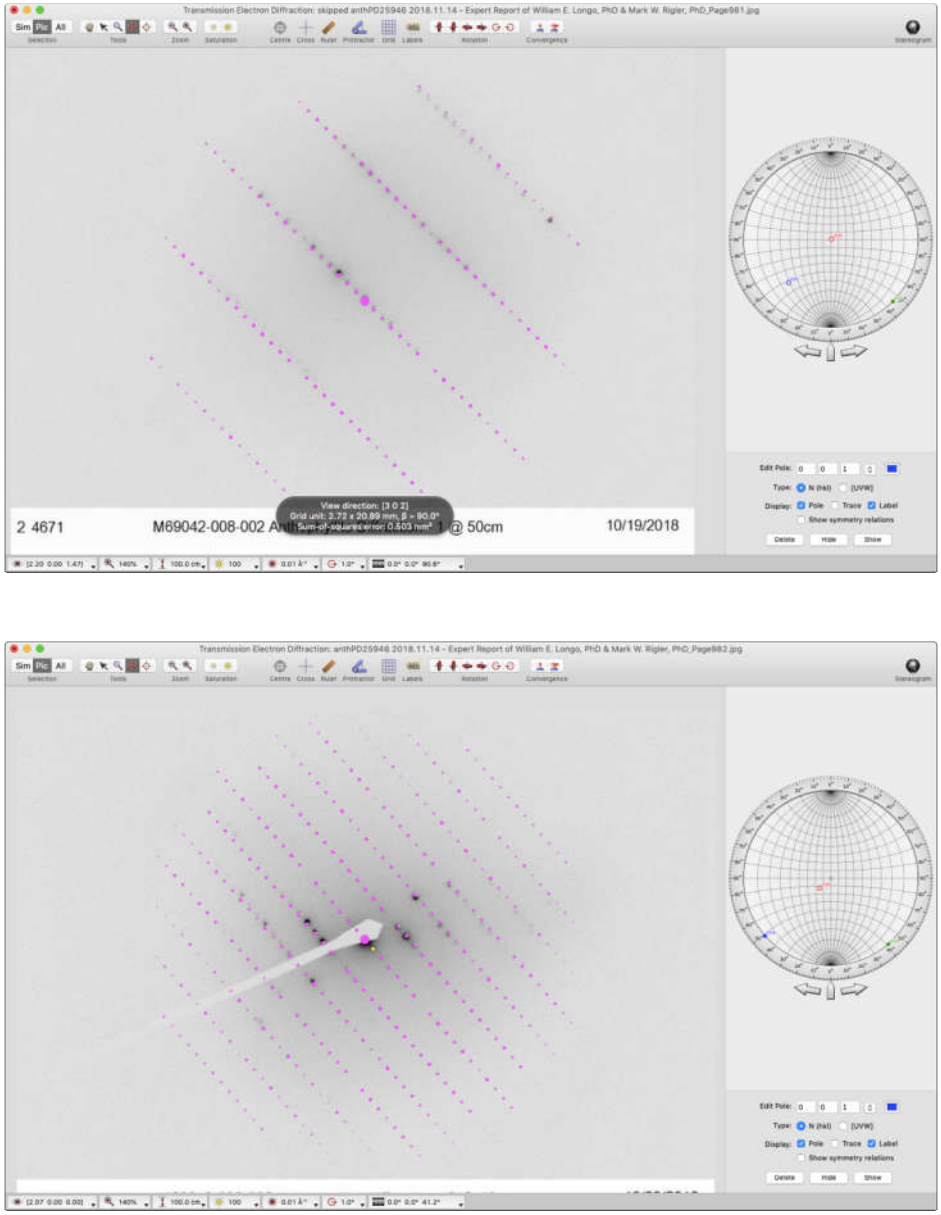


**Figure 9b.** Diffraction review of the two SAED patterns from M69042-008-002. *Top:* Index diffraction 1 indexed to [302] clinojimthompsonite. *Bottom:* Index diffraction 2 as [100] clinojimthompsonite. Spacings of the tight reflections are 13.2Å, this measurement is inconsistent with either monoclinic or orthorhombic amphibole.

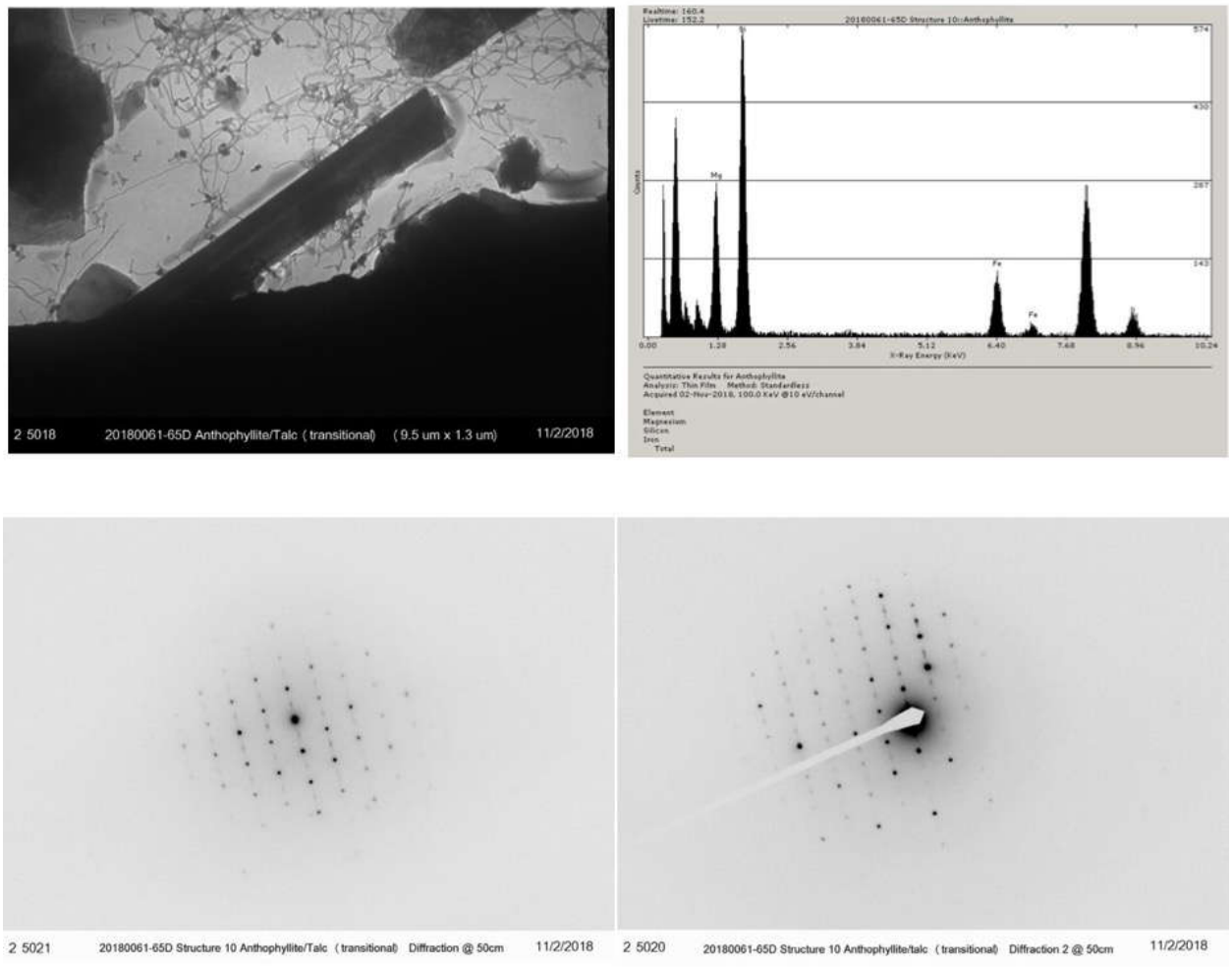


**Figure 10a.** Image, EDS, and two SAED patterns from structure 10 from 20180061-65D. Dr. Longo misidentified as a transitional structure of talc/anthophyllite.

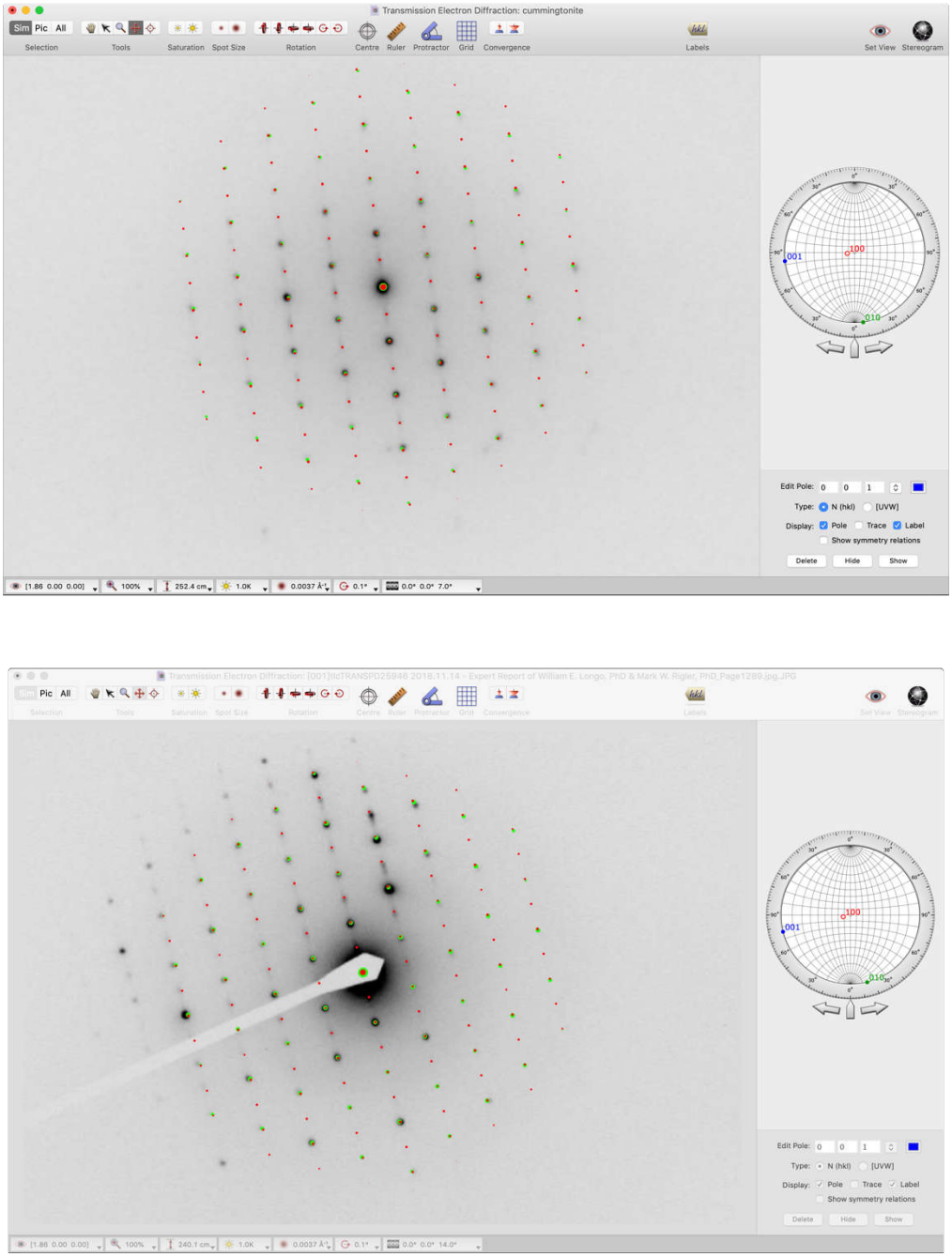


**Figure 10b.** Diffraction review of the two SAED patterns from structure 10 20180061-65D. *Top:* Index diffraction 1 indexed to [100] cummingtonite (red) and [001] talc (green). *Bottom:* Index diffraction 2 as [100] cummingtonite (red) and [001] talc (green).

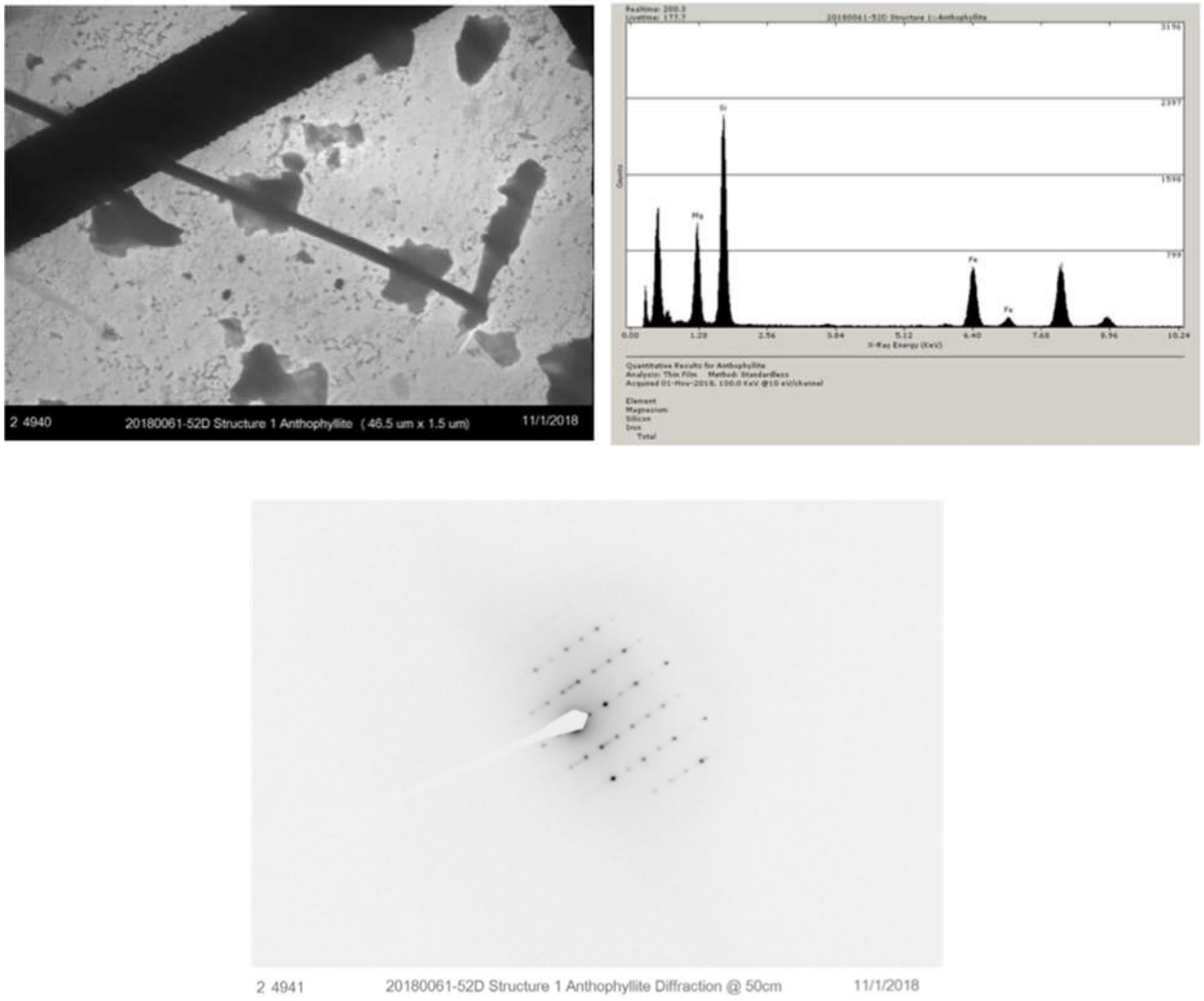


**Figure 11a.** Image, EDS, and SAED patterns from structure 1 from 20180061-52D. Dr. Longo misidentified as anthophyllite.

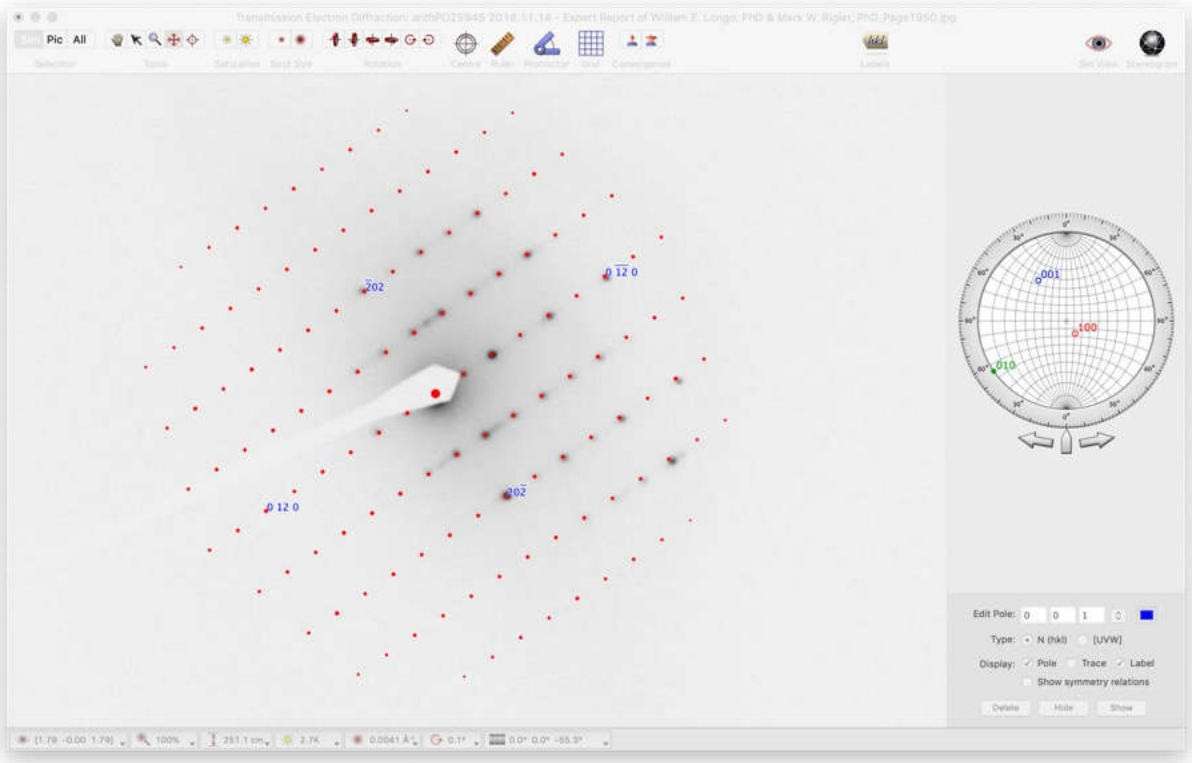


**Figure 11b.** Diffraction review of the SAED pattern from structure 1 20180061-52D. Single Crystal overlay of [101] cummingtonite (red). Streaking in between reflections along b* indicate that another phase is present, most likely talc and other wide-chain pyriboles.

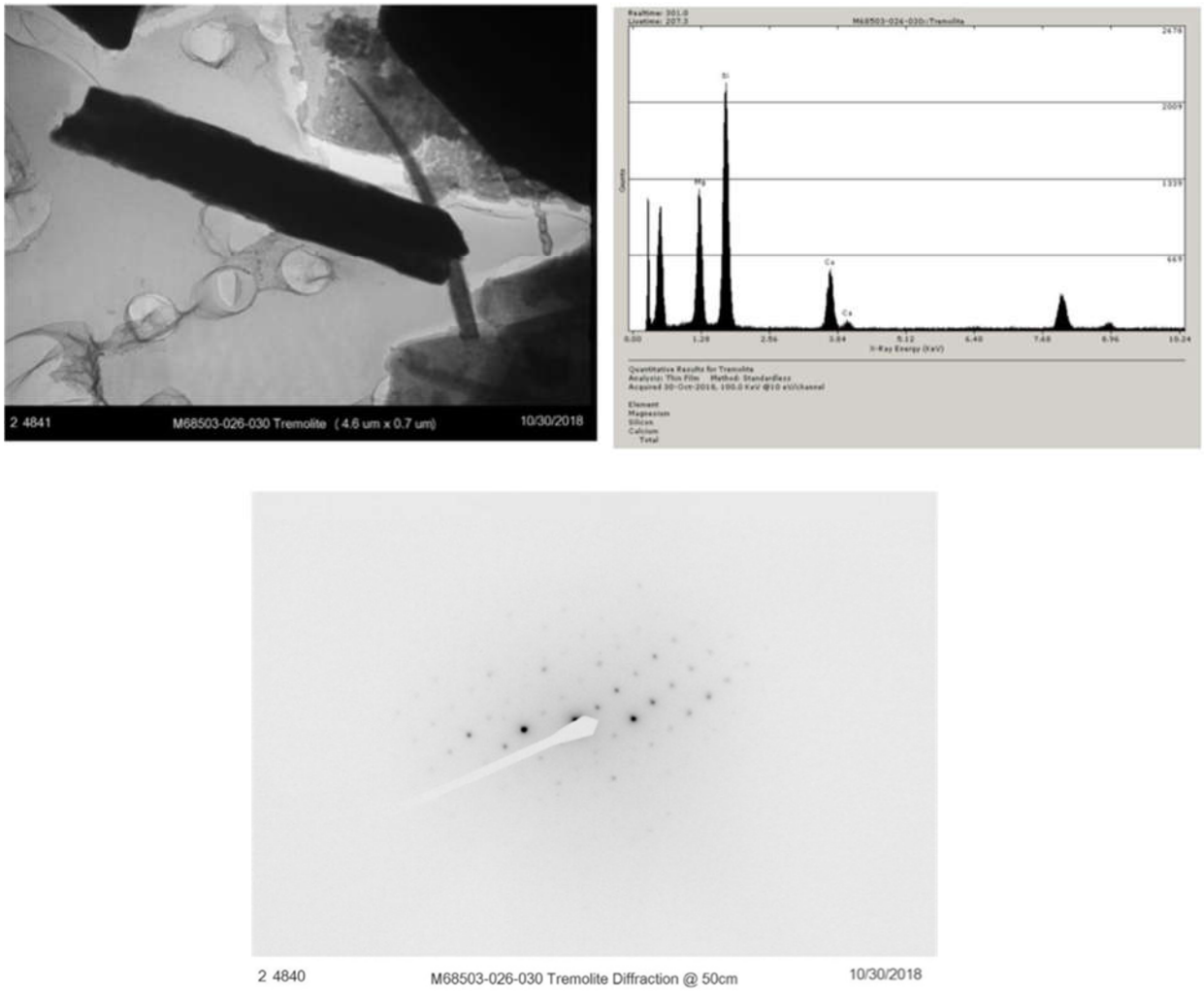


**Figure 12a.** Image, EDS, and SAED patterns from structure 030 of M68503-026. Dr. Longo misidentified as tremolite.

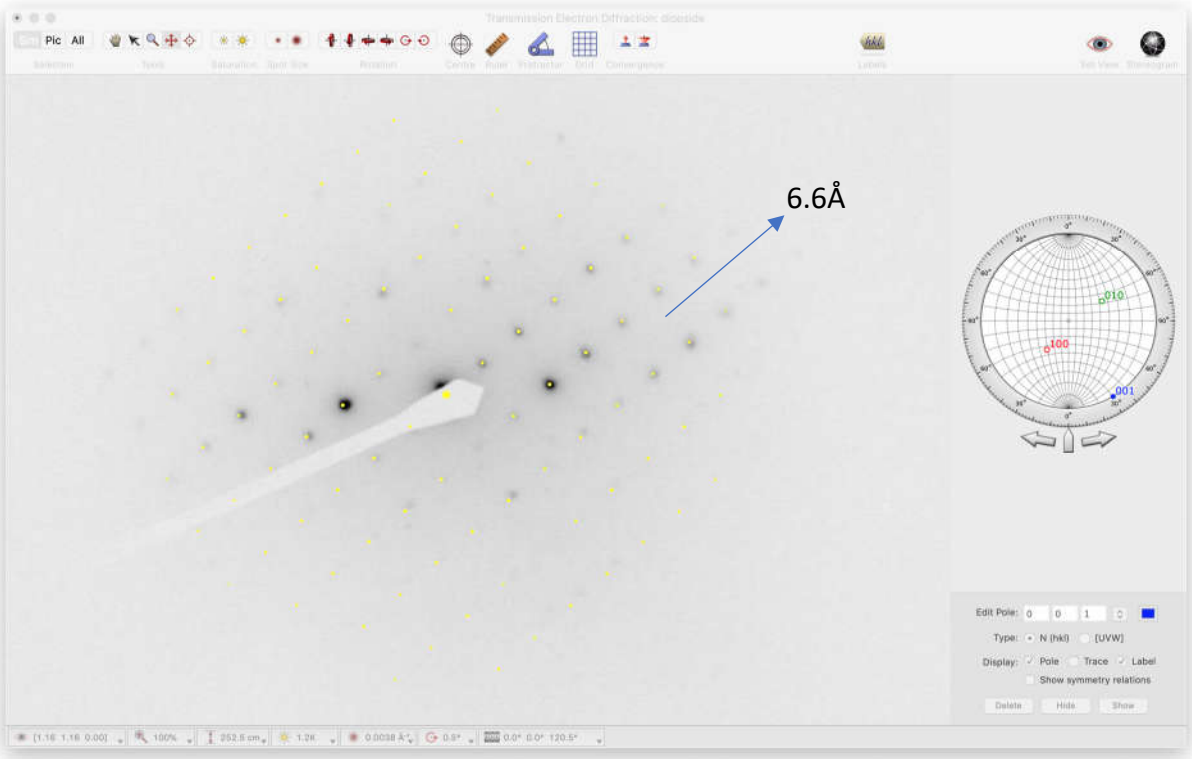


**Figure 12b.** Diffraction review of the SAED pattern from M68503-026-030. The correct index for this particle is the [110] diopside, a monoclinic pyroxene group mineral. Dr. Longo misidentified as tremolite since he only measured the row spacing as 4.92 Å. He did not measure $d_1$ which measured as 6.6 Å. Tremolite does not have a reflection with a 6.6 Å measurement.

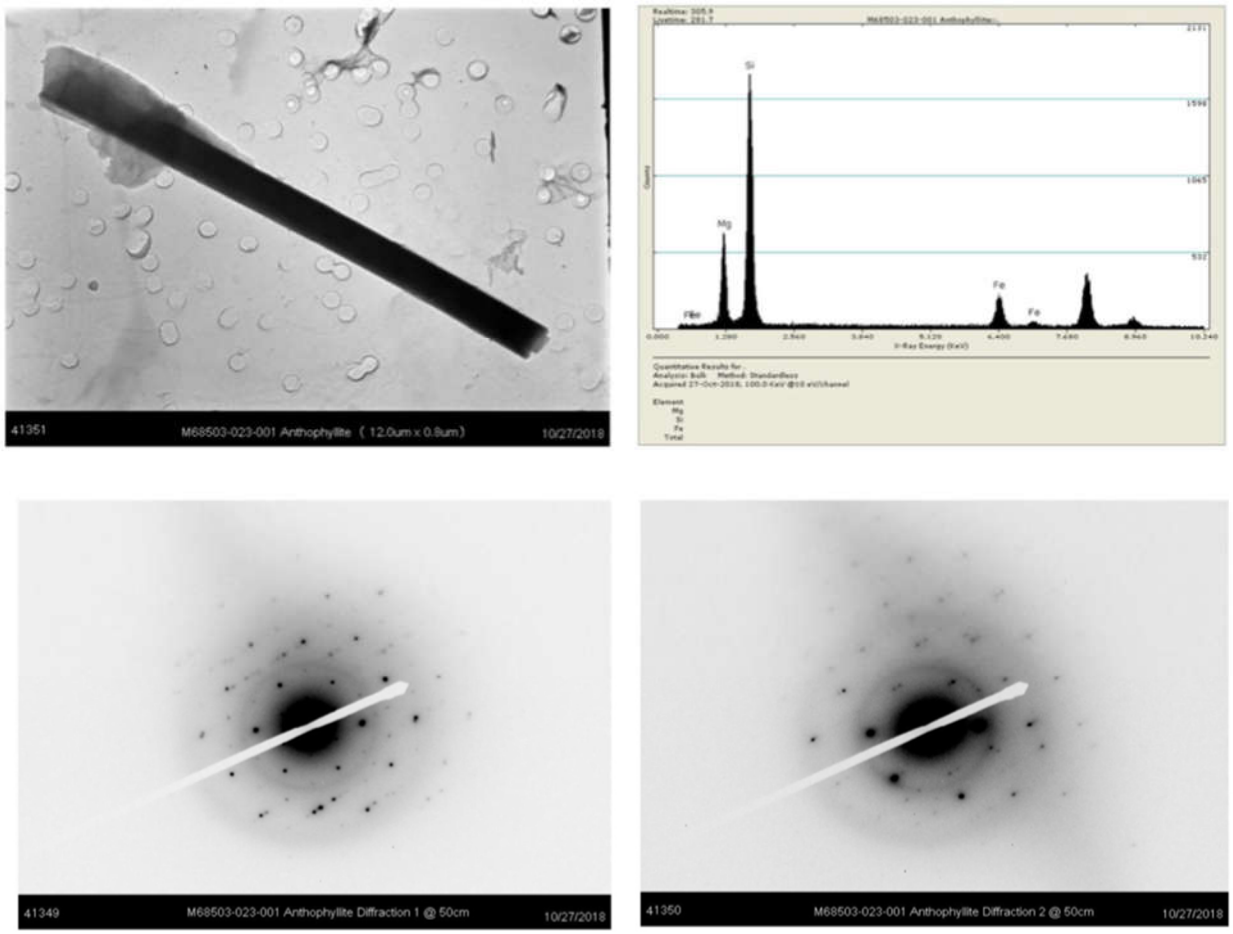


**Figure 13a.** Image, EDS, and two SAED patterns from structure 001 from M68503-023. Dr. Longo misidentified as anthophyllite. Diffraction 2 is unmeasurable.

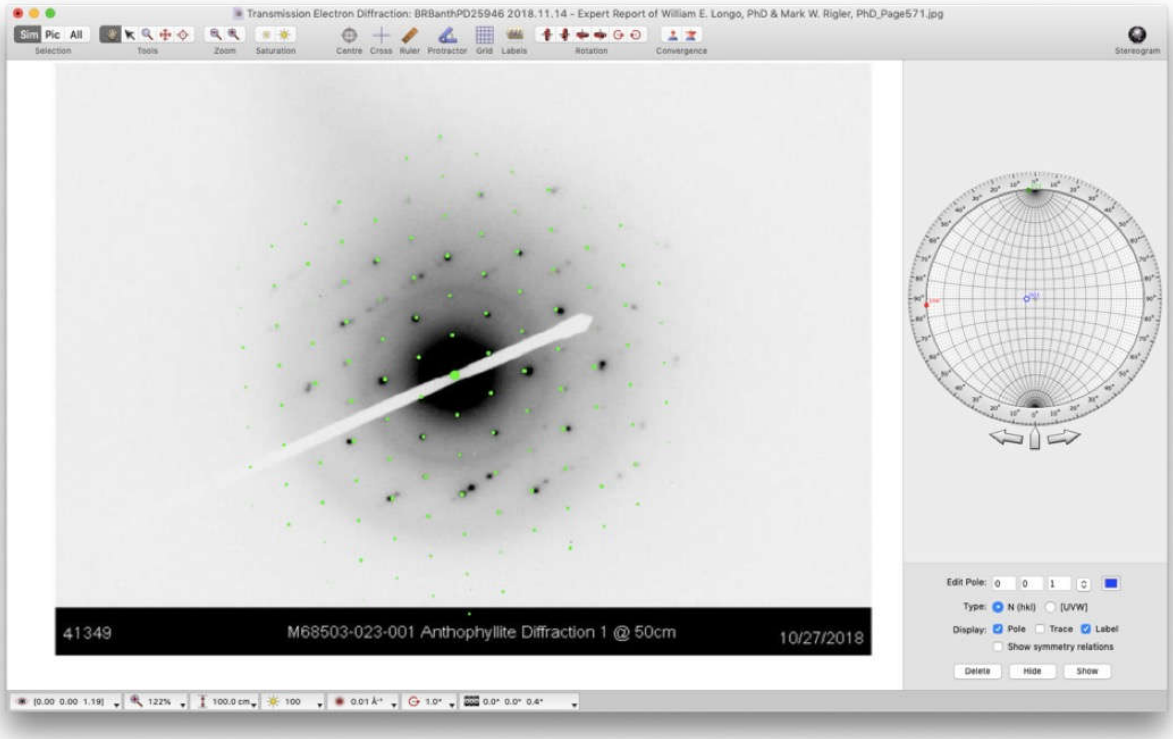


**Figure 13b.** Diffraction review of diffraction 1 from M68503-023-001. *Top:* Index diffraction 1 indexed [001] talc (green). There is another unidentified phase present but based on this limited data it cannot be identified.

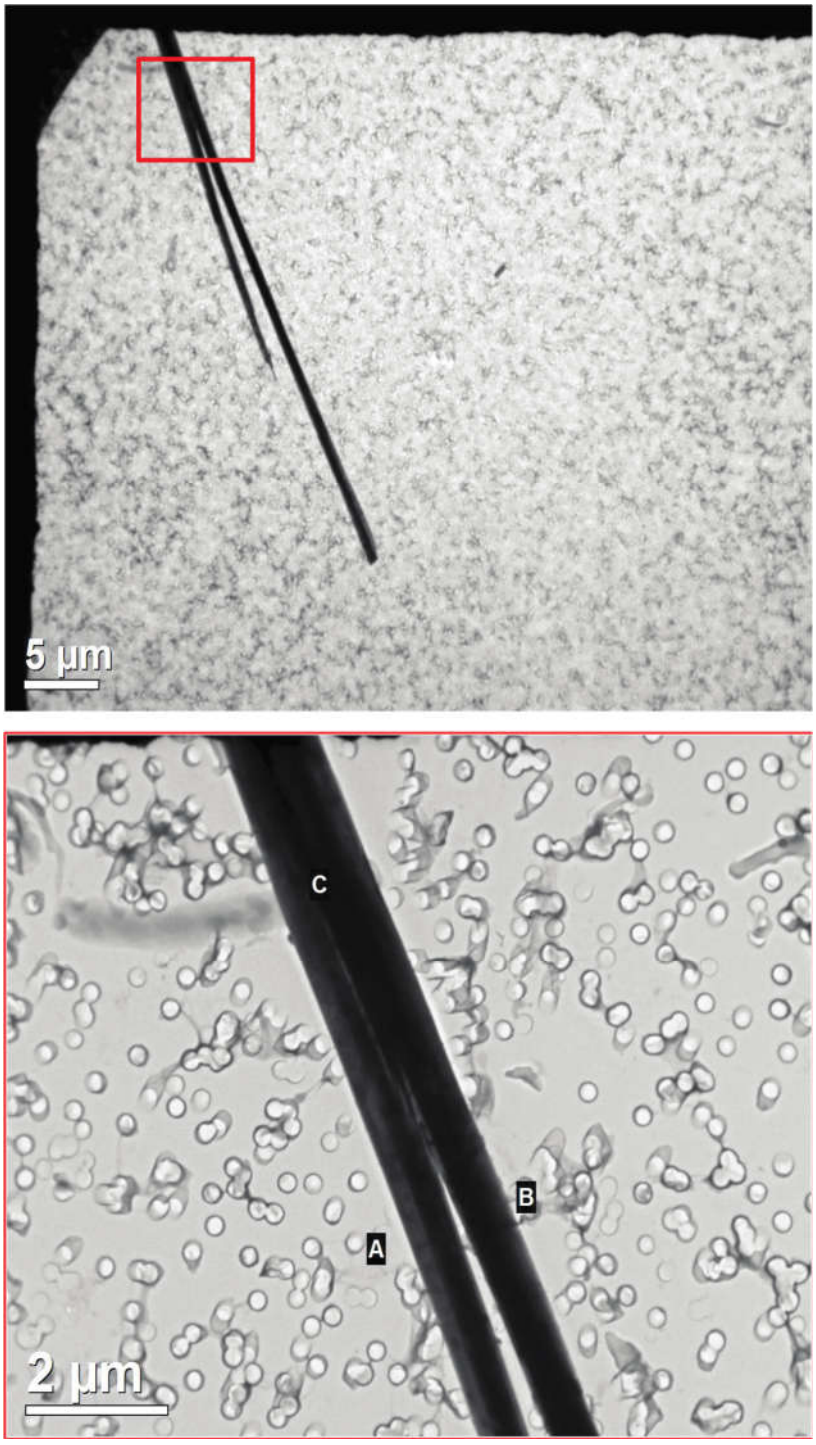


**Figure 14a.** Example of a bundle of amosite asbestos as observed by TEM. This is taken from the NIST 1866 Amosite standard reference material. In the upper image one can see the asbestos fibers splaying apart. The areas marked as A, B, and C are the areas where zone axis electron diffraction patterns were obtained and are shown and discussed in Figures 13b, Figure 13c, and Figure 13d.

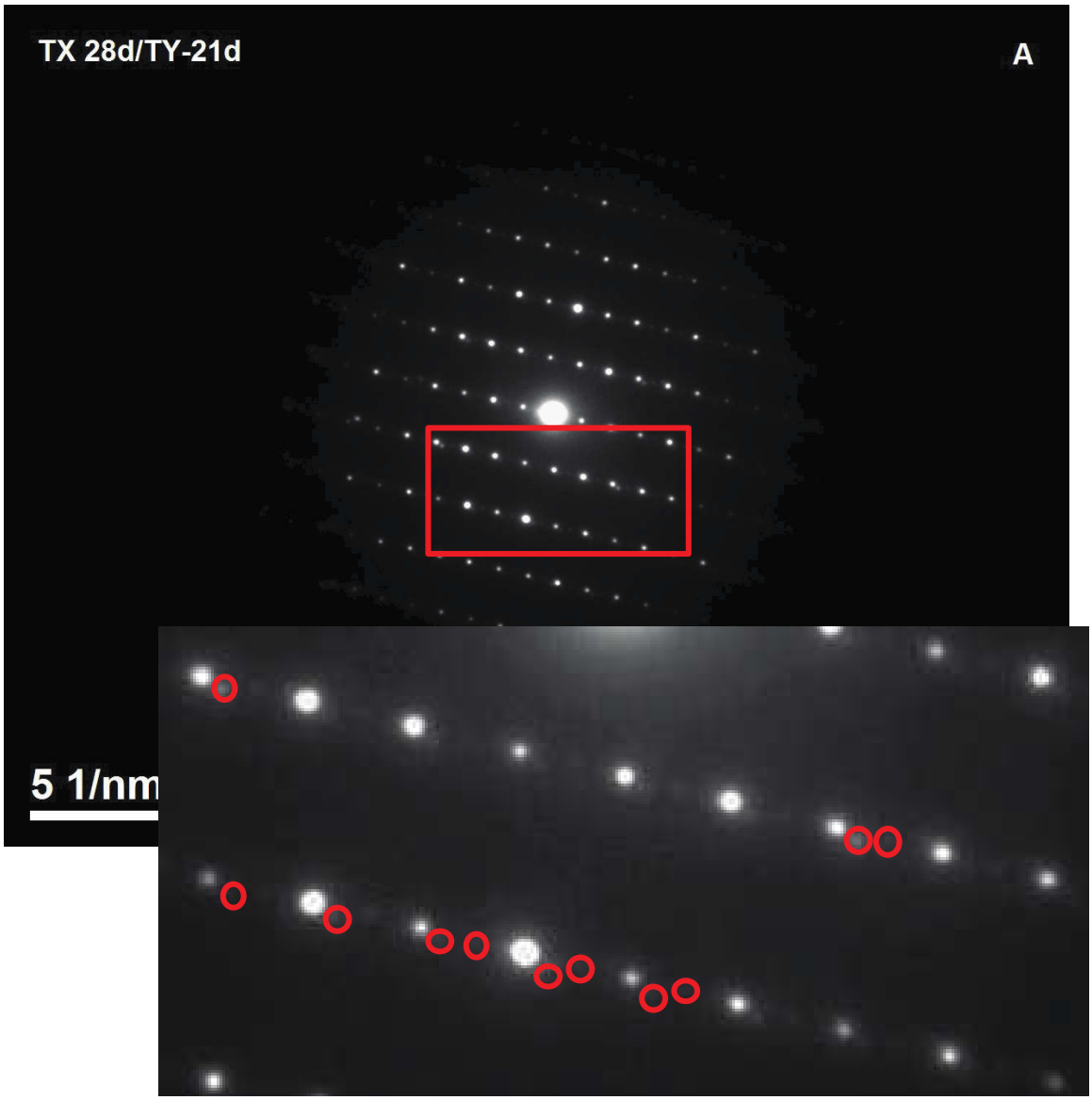


**Figure 14b.** Zone axis electron diffraction pattern from area A from Figure 13a. Note the symmetrical appearance and even intensities of the reflections. The square denotes the area of the diffraction pattern that is enlarged in the lower image. Note the presence of unsystematic reflections nearly perpendicular to the layer lines. These extra reflections are due to the polycrystalline nature of this asbestos fiber. Even at point A this particle is composed of multiple fibrils producing random diffraction patterns in perpendicular to the c crystallographic axis.

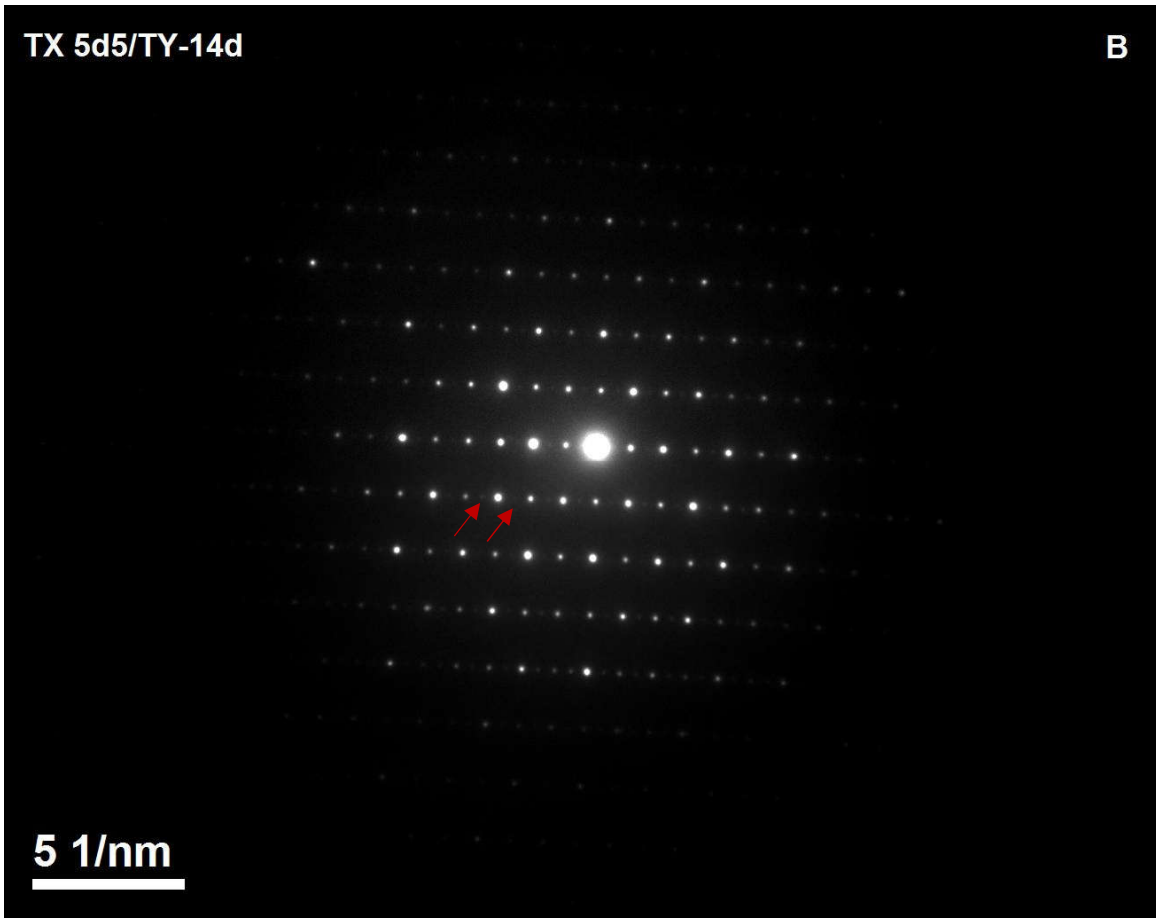


**Figure 14c.** Zone axis electron diffraction pattern from area B from Figure 13a. Note the symmetrical appearance and even intensities of the reflections. Also note the lack of any random orientation reflections as observed in Figure 13b. There are some coherent reflections of less intensity along b which are the result of a (100) twin plane in this particular amosite fiber. Nano-scale twin(s) are common in the monoclinic forms of amphibole asbestos like amosite.

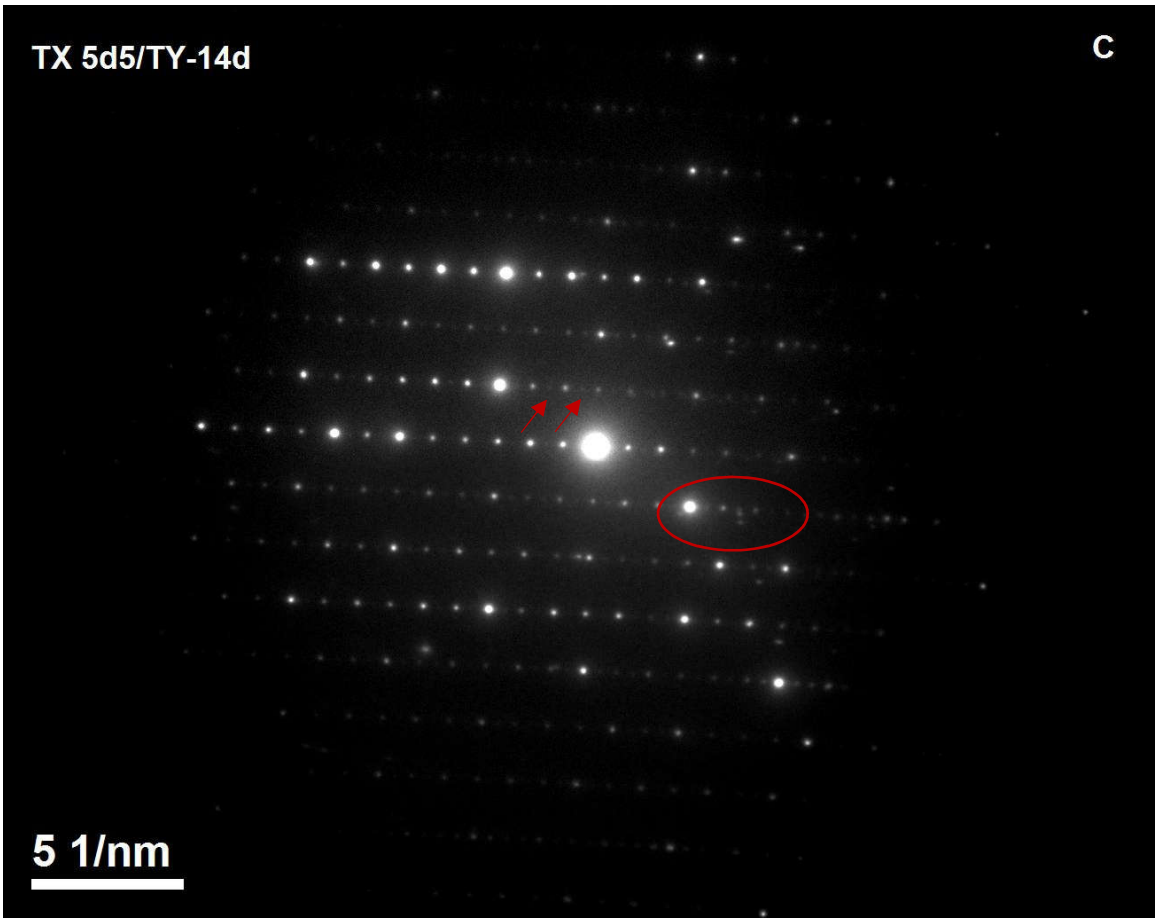


**Figure 14d.** Zone axis electron diffraction pattern from area C from Figure 13a. Note the symmetrical appearance and even intensities of the reflections. Also present are the same features observed at both locations A and B, specifically, the presence of non-coherent reflections perpendicular to the c-axis illustrated in the circle denoting the presence of multiple fibrils as shown in Figure 13b, as well as the faint coherent reflections due to the presence of the (100) twins as shown in Figure 13c.

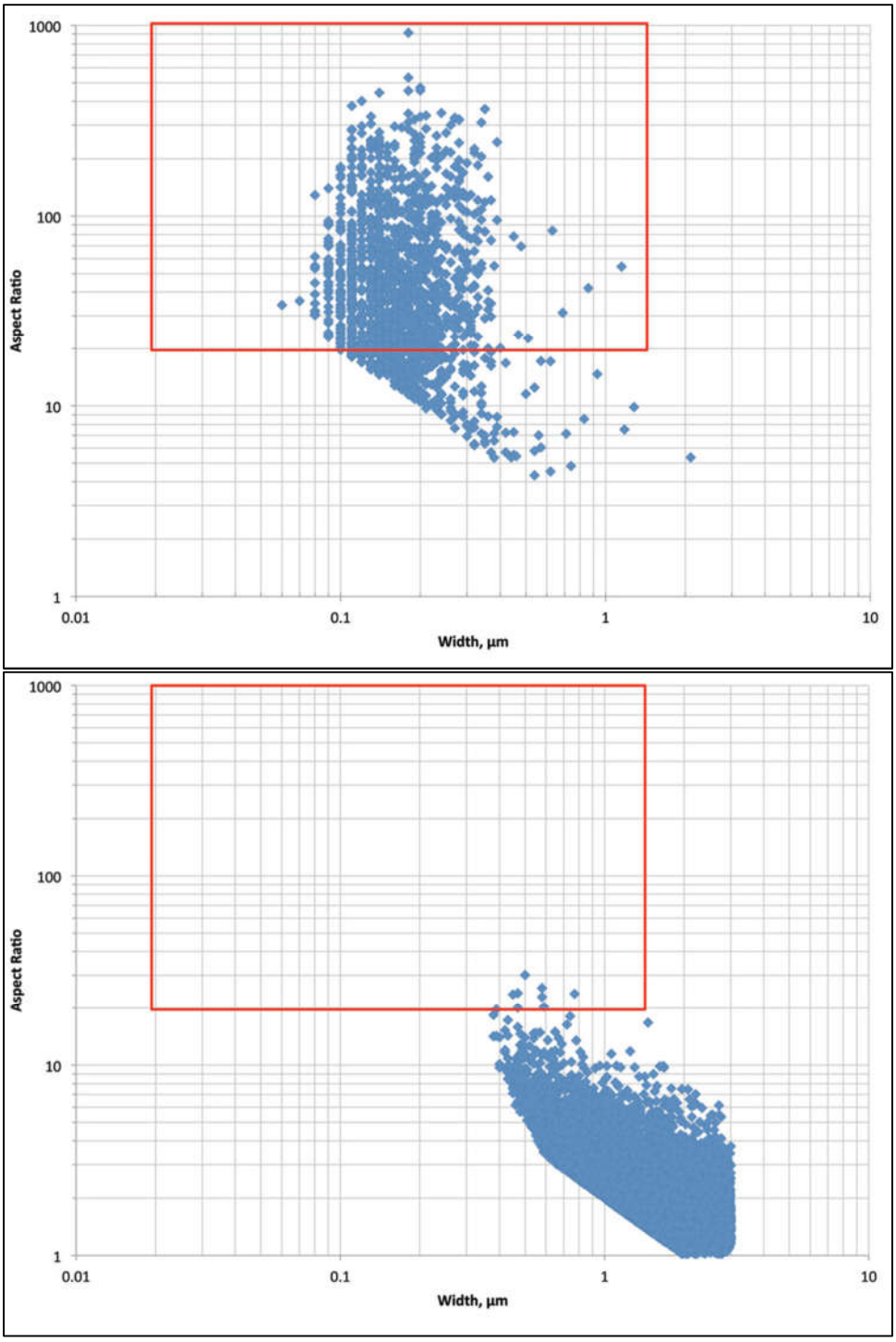


**Figure 15a.** Log aspect ratio distribution as a function of Log width for both HSE actinolite asbestos (top) and a non-asbestiform actinolite (bottom) from San Bernadino, California from Van Orden et al. 2016.

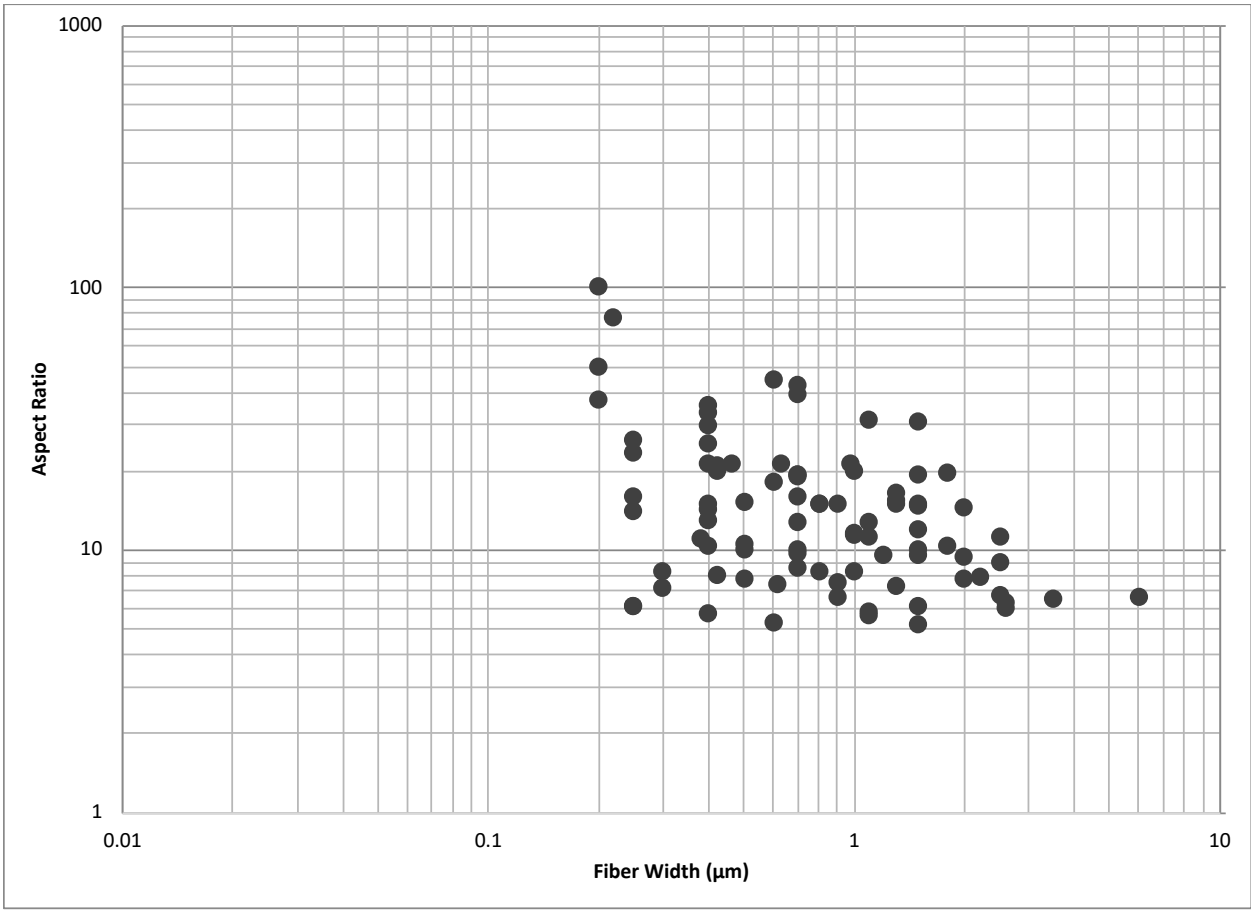


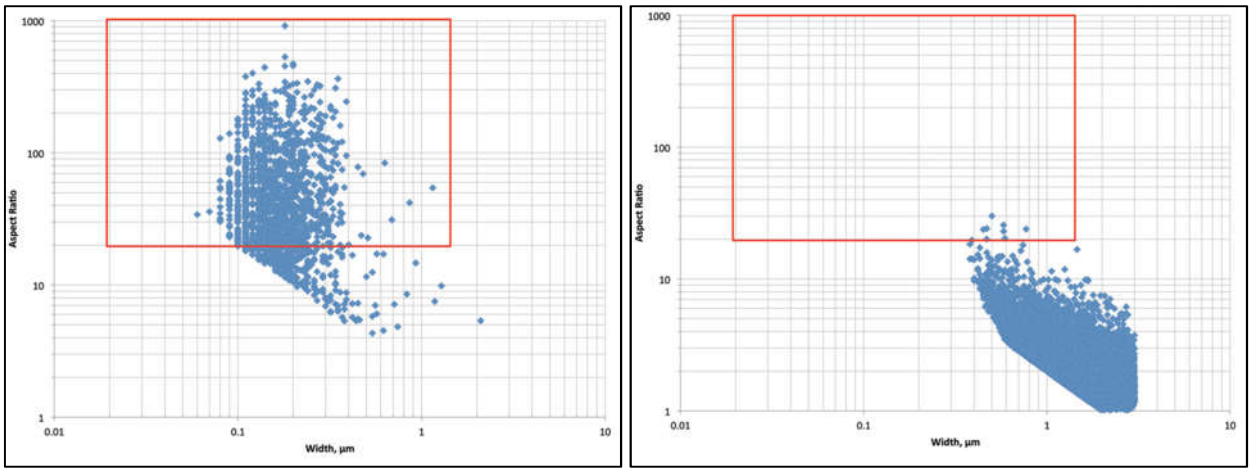


**Figure 15b.** Comparison of all "anthophyllite" TEM data for all alleged anthophyllite asbestos particles observed by Dr. Longo (top image) compared to both the population characteristics of HSE actinolite asbestos and non-asbestos actinolite shown in Figure 14a. The distribution of particles is inconsistent with the asbestiform morphology and is more consistent with non-asbestiform amphibole.

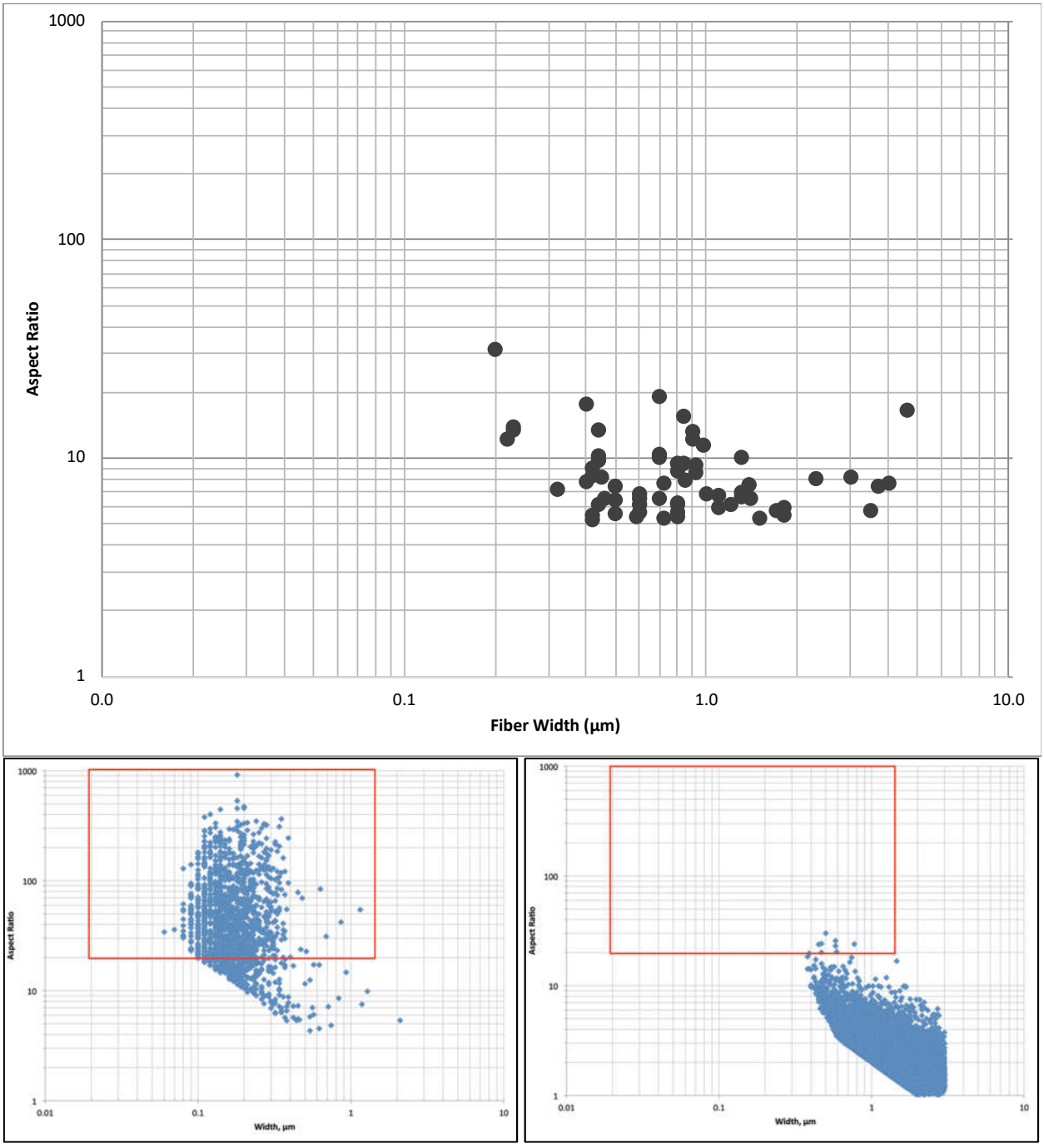


**Figure 15c.** Comparison of all TEM data for all alleged tremolite/actinolite asbestos particles observed by Dr. Longo (top image) compared to both the population characteristics of HSE actinolite asbestos and non-asbestos actinolite shown in Figure 14a. The distribution of particles is inconsistent with the asbestiform morphology.

RJ LEE GROUP
DELIVERING SCIENTIFIC RESOLUTION

**Appendix C**
**Bundle as a function of magnification**

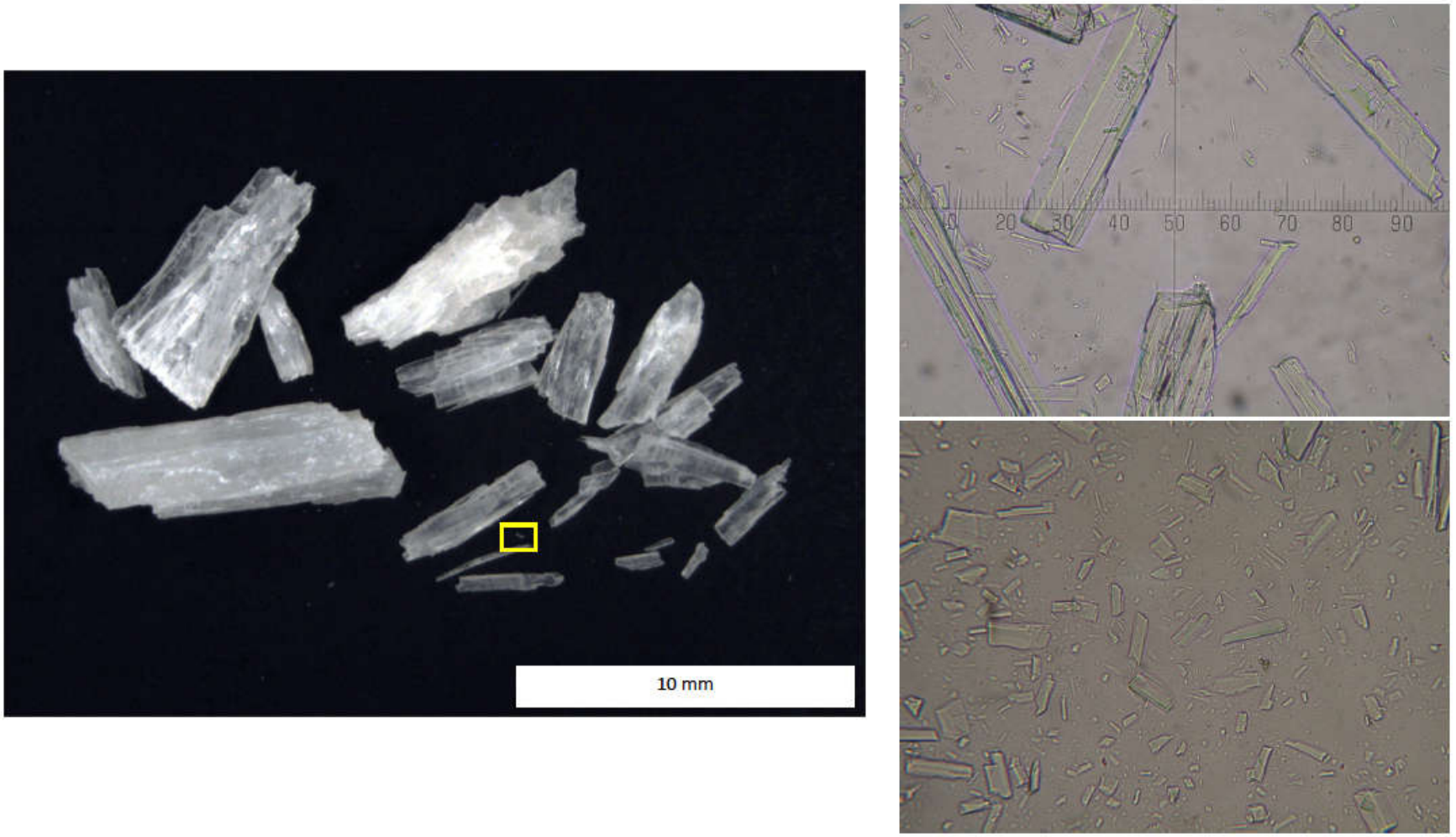


**Figure 1. Non-asbestiform amphibole morphology. The yellow box is the field of view of the pair of images on the left.**


**Figure 2. Asbestiform morphology. The yellow box is the field of view for the two images on the left.**

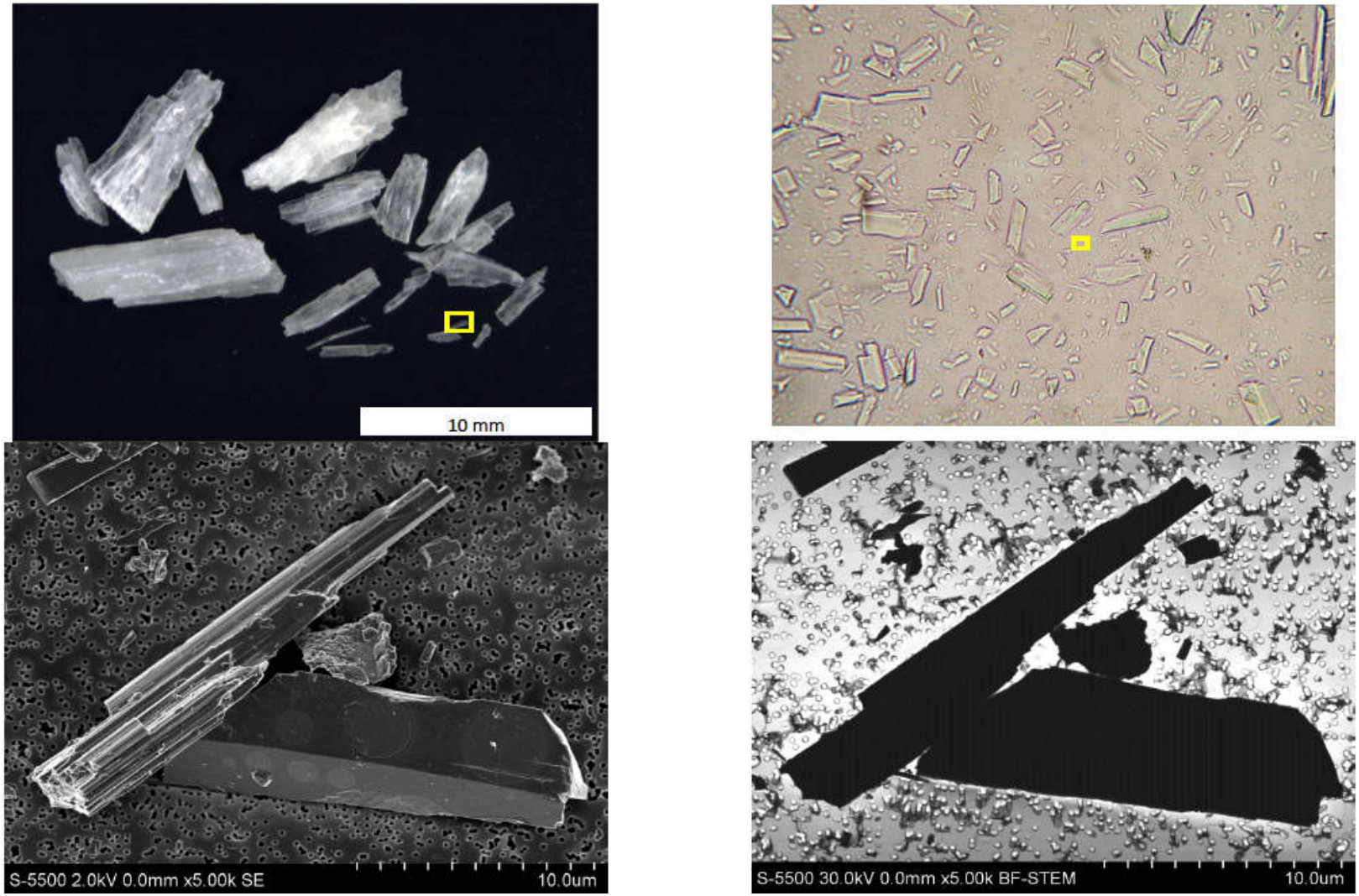


**Figure 3. Non-asbestiform morphology. The yellow box is one field of view scaled from left to right.**

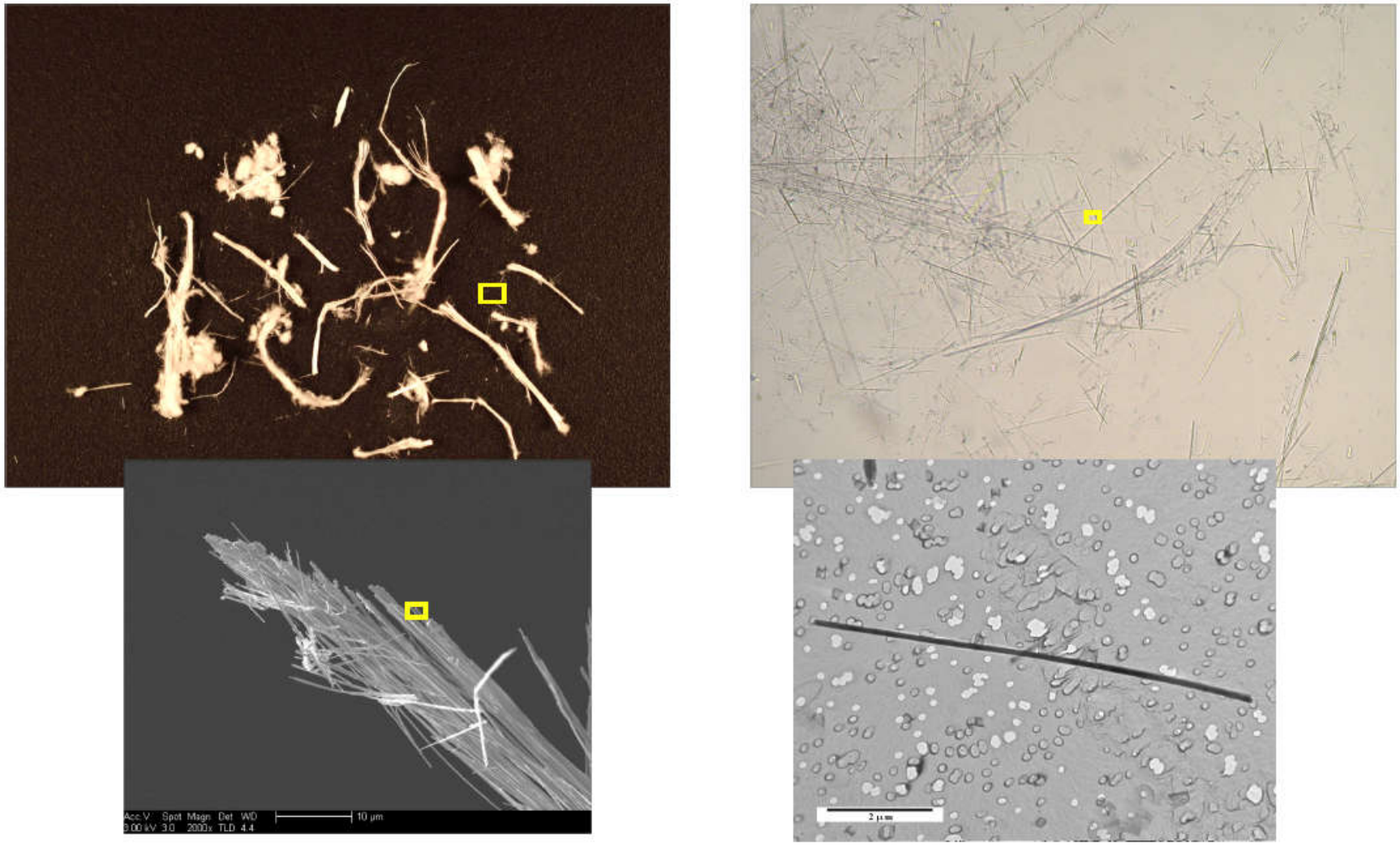


**Figure 4. Asbestifrom morphology. The yellow box is the field of view in procession from top left, top right, bottom left, bottom right.**